A protocol for the determination of absorbed dose from high-energy photon and electron beams*

Task Group 21, Radiation Therapy Committee, American Association of Physicists in Medicine‡

TABLE OF CONTENTS

Page

Preface 741

I. List of symbols and units 742

II. Introduction
- A. General considerations 743
- B. Specification of beam quality 745
- C. Dosimeters 745
- D. Buildup caps 746
- E. Dosimetry phantoms 746
- F. Absorbed-dose calibrations 747
- G. Alternate methods 747

III. The cavity-gas calibration factor N_{gas}
- A. Relationship of the dose to the gas (air) in a chamber and the exposure calibration factor 747
- B. The exposure-calibration factor, N_X 748
- C. Ratios of stopping powers and mass energy-absorption coefficients for ^{60}Co gamma rays 748
- D. Ion collection efficiency 748
- E. Wall correction factor 749
- F. Quotient of absorbed dose by collision fraction of kerma 749
- G. Fraction of ionization due to electrons from chamber wall 750
- H. Absorbed-dose calibrated ionization chambers, N_D 750

IV. Dose to the medium
- A. Spencer–Attix formulation of the Bragg–Gray relationship 750
- B. Stopping-power ratios 751
- C. Ionization recombination correction 752
- D. Replacement correction 753
- E. Ratios relative to air of mean mass energy-absorption coefficients 758
- F. Fraction of ionization due to electrons from the chamber wall 758
- G. The ^{60}Co buildup cap and in-phantom measurements 758

V. Dosimetry phantoms
- A. Materials and dimensions 758
- B. Depth of calibration 759
- C. Scaling factors and dose transfer, plastic to water (photons) 759
- D. Scaling factors and dose transfer, plastic to water (electrons) 761

VI. Calibration of ^{60}Co teletherapy units
- A. In-air calibration 762
- B. Water-phantom calibration using N_D 762

VII. General considerations
- A. Choice of ionization chamber 762
- B. N_{gas} for plane-parallel chambers 763
- C. Dose to tissues 763
- D. Alternate dosimetric methods 763
  1. Calorimeters 763
  2. The Fricke ferrous-sulfate dosimeter 763
  3. Independent ionization chambers 763

VIII. Application of the Protocol
- A. Summary 764
- B. Application 764

References 771

PREFACE

The success or failure of radiation therapy can depend upon the accuracy with which a dose prescription is fulfilled. For many diseases the required accuracy is not known; for others, the outcome of treatment depends upon tumor doses that do not vary by more than $\pm$ 5% about the optimum.[1] The establishment of tumor-cure probabilities, optimized time-dose schedules, and radiobiological efficiencies requires that the systematic uncertainties in dosimetry be made considerably smaller than the uncertainties in measuring tumor volume and response. This necessitates that improved accuracy be sought in the dosimetry of high-energy photon and electron beams, which is the subject of this Protocol. Also, the comparative clinical assessment of therapeutic radiations other than x rays and electrons, such as neutrons, protons, pions, and heavy ions, emphasizes further the necessity for improving the accuracy of photon and electron dosimetry. The ICRU[2] estimates the uncertainty in high-energy x-ray dosimetry, performed with a calibrated ionization chamber, to be $\pm$ 3.3%, however, recent reports on this subject[3–6] suggest that the uncertainty is higher than this. There are no comparable data for electron beams, but the uncertainties are likely to be even greater because of the pronounced dependence of electron spectra, and consequently stopping-power ratios, on depth. As the conceptual aspects

*Reprints can be ordered from the AAPM Headquarters, 335 East 45th Street, New York, NY 10017.

‡Task Group 21, Radiation Therapy Committee, AAPM: Robert J. Schulz, *Yale University, Chairman*; Peter R. Almond, *University of Texas, M. D. Anderson Hospital*; John R. Cunningham, *University of Toronto, Princess Margaret Hospital*; J. Garrett Holt, *Memorial Sloan–Kettering Cancer Center*; Robert Loevinger, *National Bureau of Standards*; Nagalingam Suntharalingam, *Thomas Jefferson University*; Kenneth A. Wright, *Massachusetts Institute of Technology*; Ravinder Nath, *Yale University, Consultant*; Geoffrey D. Lempert, *Yale University, Research Associate*.

 0094-2405/83/060741-31$01.20

of radiation dosimetry are advanced, and physical data and measuring instruments are improved, it is incumbent upon the radiological physics community to adopt these improvements in order to reduce the uncertainty in the dose calibrations of radiation therapy machines. The purpose of this Protocol is to describe methods and provide data that will permit radiological physicists to determine absorbed dose more accurately than has heretofore been possible.

Prior to 1980, there were a number of codes, protocols, and reports by national and international organizations which provided physicists with a systematic approach to the dosimetry of high-energy photons and electrons.[7-10,54] Although a variety of dosimetric methods are discussed in these documents, a common characteristic of all of them is the use of an ionization chamber having an exposure-calibration factor for ^{60}Co gamma rays or 2-MV x rays traceable to a national standards laboratory. By application of the exposure-calibration and appropriate dose-conversion factors, generally known as C_λ and C_E, in-phantom ionization measurements for high-energy radiations may be translated to absorbed dose. The method of the calibrated cavity[10] has provided medical physics and radiotherapy for almost two decades with a relatively simple and accurate means of dosimetry, and one that provided an acceptable degree of uniformity in dose delivery the world over.

It is inevitable that concepts change, and data and instrumentation are refined. The method of the calibrated cavity is totally dependent upon the ^{60}Co exposure calibration to specify what in the last analysis is the dose to the air in the chamber, and ignores how this parameter is affected by the composition and dimensions of the chamber. When C_λ is used for x-ray dosimetry, the tacit assumptions are made that the chamber is of a water-equivalent composition, and that the same replacement factor applies to all chambers regardless of the x-ray energy or the depth at which the measurement is made. When C_E is used for electron dosimetry, the assumption is made that the chamber is of an air-equivalent composition, and that an electron perturbation correction is the only depth-dependent correction that need be applied. Task Group 21 of the Radiation Therapy Committee, AAPM, was formed for the purpose of reviewing both the concepts and data employed for high-energy dosimetry, and to make revisions as required. It was recognized early that certain pitfalls could be avoided if both photon and electron dosimetry were treated as parts of the same overall problem. It was also recognized that the physical characteristics of the ionization chambers employed for clinical dosimetry, as well as mismatches between the chamber wall and phantom, must be taken into account if the accuracy of dosimetry were to be improved. The revised Protocol for high-energy dosimetry, which is presented below, departs most markedly from the earlier protocols in these respects.

Those aspects of existing protocols that the Task Group found inconsistent with the requirements of logical development and accurate dose determination are the following:

First, the concept of in-phantom measurement of exposure at the calibration energy, a concept that provides the logical basis for several derivations of dose-conversion factors,[7-10] is subject to question because in-phantom measurement of exposure requires that the in-air exposure calibration factor of the ionization chamber (with buildup cap) remain constant regardless of the depth and field size employed for the in-phantom measurement. For ^{60}Co gamma rays, about 20% of the dose to water at a depth of 5 cm and a field size of 10×10 cm^2 is contributed by scattered, energy-degraded photons. Therefore, it is necessary for the ionization chamber (with buildup cap) to have a constant exposure-calibration factor down to photon energies of approximately 200 keV.

Second, the generally accepted values of the dose-conversion factors for photons (C_λ) and electrons (C_E) do not agree for comparable in-phantom electron spectra produced by photon and electron beams.[3]

Third, the replacement factor, which is a function of chamber dimensions and the gradient of the depth-dose curve (Sec. IV D), is incorrectly treated as a constant which is independent of these parameters.

Fourth, differences in the composition of the chamber wall and dosimetry phantom, which affect the dose from x rays, are not taken into account (Sec. IV A).

These criticisms are addressed in the Protocol, and new methods and data are provided to circumvent or satisfy each one.

I. LIST OF SYMBOLS AND UNITS

α	Fraction of ionization due to electrons from the chamber wall
A_{ion}	Ion-collection efficiency in the user's chamber at the time of ^{60}Co exposure calibration at NBS or an ADCL
A_{repl}	A correction for replacement of water by the user's chamber at the time of ^{60}Co absorbed-dose calibration at NBS or an ADCL
A_{wall}	Correction for attenuation and scatter in the wall and buildup cap of the user's chamber when exposed in air to ^{60}Co gamma rays
β	Quotient of absorbed dose by the collision part of kerma
Δ	Cutoff energy in Spencer–Attix formulation of the Bragg–Gray equation (keV)
$d_{\max}$	Depth on the central axis at which an ionization chamber gives the maximum reading, for electron and photon beams (cm or g/cm^2)
d_{50}	Depth on the central axis at which an ionization chamber reads 50% of maximum, for electron beams (cm or g/cm^2)
D_{gas}	Absorbed dose to the gas (air) in the chamber (Gy)
D_{med}	Absorbed dose to the phantom medium at the position of the chamber center, with the chamber replaced by the medium (Gy)
D_{water}	Absorbed dose to water at the position of the chamber center, with the chamber replaced by water (Gy)
$\overline{E}_z$	Mean electron energy at depth of measurement (MeV)
$\overline{E}_0$	Mean incident energy of an electron beam (MeV)
$\phi_{\text{med}}^{\text{water}}$	A factor that relates electron fluence in water to that at a comparable point in a different medium

J_{gas} Specific charge in the gas (air) of the chamber (C/kg)
k Charge produced in air per unit mass per unit exposure (2.58×10^{-4} C kg^{-1} R^{-1})
$\bar{L}/\rho$ Mean restricted collision mass stopping power
M Electrometer reading normalized to 22 °C and one standard atmosphere (C or scale division)
N_X Exposure calibration factor (R/C or R/scale division) uncorrected for ion recombination
N_D Absorbed-dose calibration factor (Gy/C or Gy/scale division) uncorrected for ion recombination
N_{gas} Cavity-gas calibration factor (Gy/C or Gy/scale division)
P_{ion} Ion-recombination correction factor applicable to the calibration of the user's beam
P_{repl} A factor that corrects for replacement of phantom material by an ionization chamber
ρ Mass density of cavity gas (air) at time of measurement (kg/m^3)
R_p Practical range of an electron beam; the depth of intersection of a line drawn tangent to the depth-dose curve at the point of maximum slope and a line extrapolated from the bremsstrahlung tail (Fig. 6)
$(\bar{S}/\rho)$ Mean unrestricted collision mass stopping power
SDD Source–detector distance (cm)
SSD Source–surface distance (cm)
$\bar{\mu}_{en}/\rho$ Mean mass energy-absorption coefficient
V Chamber collecting volume (m^3)
W/e Mean energy expended per unit charge in air at usual humidity ($\simeq$33.7 J/C)
X Exposure at position of chamber center, with chamber replaced by air (R)
z/R_p Depth of penetration of an electron beam, expressed as a dimensionless fraction of the practical range

Physical quantity	Unit name	Unit symbol
Length	meter	m
Mass	kilogram	kg
Time	second	s
Time	minute	min
Thermodynamic temperature	Kelvin	K
Celsius temperature	degree Celsius	°C
Pressure	pascal	Pa
Pressure	millimeters of mercury	mmHg
Energy	joule	J
Energy	electron volt	eV
Electric potential	volt	V
Electric charge	coulomb	C
Absorbed dose	gray	Gy (= J/kg)
Exposure	roentgen	R
Electron concentration	electrons per cubic centimeter	e$^-$/cm^3
Mass per unit area	grams per square centimeter	g/cm^2

Conversion factors

Thermodynamic temperature (K) = Celsius temperature (°C) + 273.16

Pressure (Pa) = Pressure (mmHg) $\times$ 133.3

Energy (J) = Energy (eV) $\times 1.602\times10^{-19}$

Electric charge (C) = Electric charge (esu) $\times 3.336\times10^{-10}$

Air collision kerma (kinetic energy released per unit mass) (Gy) =

$$\frac{\text{Exposure (R)} \times W/e\text{(J/C)} \times 2.58\times10^{-4}}{(1-g)},$$

where g is the fraction of the initial electron kinetic energy expended in radiative interactions.

II. INTRODUCTION

A. General considerations

The purpose of this Protocol is to provide radiological physicists with an accurate method for determining the dose to water from the high-energy photon and electron beams used for radiation therapy, i.e., ^{60}Co gamma rays, x rays with maximum energies in the range of 2–50 MeV, and electron beams with mean incident energies in the range of 5–50 MeV. The approach of this protocol is markedly different from earlier protocols that have been widely followed in the United States, such as SCRAD[10] and ICRU Report No. 21,[8] in that (a) the response of an ionization chamber is characterized by a new parameter N_{gas} that is a function of a variety of chamber-dependent parameters in addition to the ^{60}Co exposure-calibration factor; (b) polystyrene and acrylic plastics as well as water are recommended for primary dosimetry phantoms; (c) all chamber-dependent and radiation-dependent parameters remain explicit in the dose calculations.

The flow diagram, Protocol Procedures and Section References, shown on the following page, was prepared to show the sequence of, and thereby place into perspective, each component of the Protocol. The major components are listed in the left-hand column, and the physical parameters and other dosimetric data that relate to each of the components, and section references for these data, are listed in the right-hand column.

(A) A ^{60}Co calibration factor for the user's ionization chamber is a prerequisite for application of the Protocol. Although the ^{60}Co factor is not a major component of the Protocol, it is given a position of prominence in the flow diagram so as to assure the reader that this national reference standard, which in no small part is responsible for the high level of uniformity in radiation-therapy dosimetry, continues to play an essential but less explicit role.

(B) The cavity-gas calibration factor N_{gas} is the dose to the gas (air) in the chamber per unit electrometer reading. It is a constant for all radiation qualities for which the average en-

Protocol Procedures and Section References

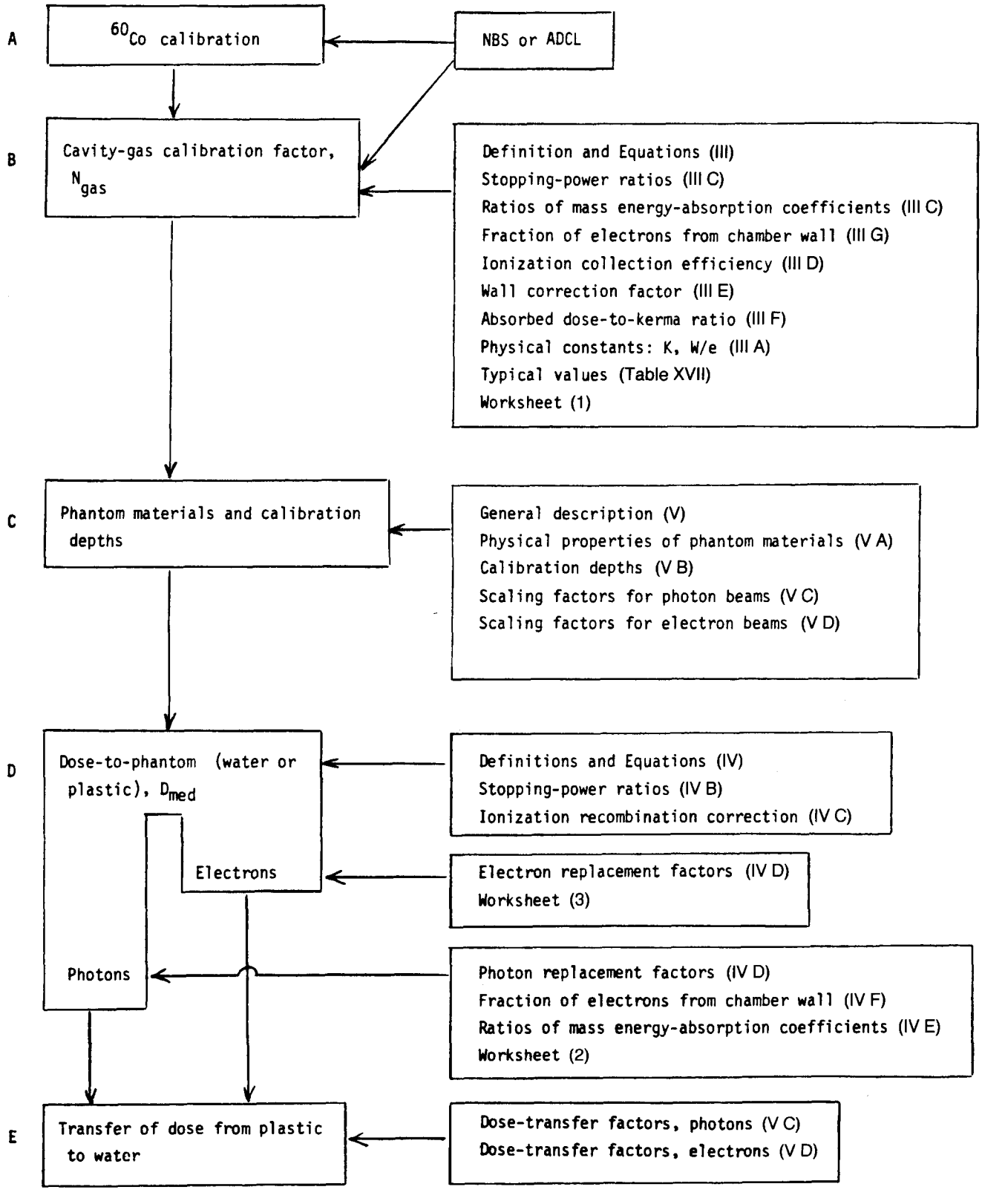

ergy expended in the production of one ion pair (W) is the same as that for ^{60}Co gamma rays (33.7 eV). This is the case for the radiations covered in this Protocol as well as for x rays with energies as low as 10 keV. The cavity-gas calibration factor can be obtained from the National Bureau of Standards (NBS) or an Accredited Dosimetry Calibration Laboratory (ADCL) at the time of the ^{60}Co exposure calibration, or it may be calculated according to the theory and equations of Sec. III using the N_{gas} Worksheet of Sec. VIII. The calculation of N_{gas} need be made only once, and subsequently only if the ^{60}Co exposure calibration were to change.

(C) The user may choose any of three materials for a dosimetry phantom: water, polystyrene, or acrylic plastic. Recommended calibration depths for water phantoms are given in Sec. V. When polystyrene or acrylic phantoms are used for x-ray dosimetry, the calibration geometry must be adjusted so that the photon fluence at the dosimeter is the same as that at the calibration depth in a water phantom. When plastic phantoms are used for electron dosimetry, the geometry is the same as for a water phantom, however, corrections for differences in the electron fluence in plastic compared with water will be required. There are advantages and disadvantages to each of these materials. As water is the reference material for dose calibrations, the additional step of transferring dose to plastic to dose to water is avoided by the use of a water phantom. On the other hand, water phantoms take more time to make ready, are inconvenient by comparison with plastic phantoms, require a waterproof chamber, present difficulties in accurate repositioning of the chamber, and hydrostatic pressure may cause volume or pressure changes in some types of chambers. It is recommended that the user choose a dosimetry phantom that, based upon the data provided in the Protocol and his own unique requirements, will yield the most accurate and reproducible dosimetry for his radiation beam.

(D) When ionization-chamber measurements are made in phantom, the product of N_{gas} and the electrometer reading is the dose to gas in the chamber due to the radiation fluence at the measurement point. The dose to the phantom material that replaces the chamber when it is removed from the phantom is given by the product of the dose to gas, the ratio of stopping powers of the phantom material to air, and factors that account for phantom replacement and ionization recombination. The theory and data for calculating dose to phantom are given in Sec. IV and Worksheets for x-ray and electron beam dosimetry are in Sec. VIII.

(E) When plastic dosimetry phantoms are used, the theory and data of Sec. IV enable the user to determine the dose to plastic. Having followed the irradiation procedures recommended in Sec. V, the photon fluence at the measurement point in the plastic phantom is the same as would be obtained at the calibration depth in a water phantom. When photon fluences are equal, the dose to water is related to the dose to plastic by the ratio of their average mass energy-absorption coefficients. After correcting the dosimeter response for the lower electron fluence in polystyrene and acrylic plastics, the dose to water is given by the product of the dose to plastic and the ratio of their unrestricted mass collisional stopping powers. These ratios, referred to as dose transfer factors, for x rays and electrons are given in Sec. V.

B. Specification of beam quality

The ratio of average stopping powers, which is required for the calculation of dose to the phantom material, is a function of the spectrum of electrons at the point of measurement, and this spectrum, in turn, is a function of the energies of the incident x rays or electrons. As the x-ray or electron spectra produced by accelerators operating at the same energy may differ significantly, the selection of stopping-power ratios based upon the console reading of beam energy can result in a systematic error in dosimetry. The Protocol recommends that indices of beam quality be determined from in-phantom depth-ionization measurements.

For x rays, it is assumed that the secondary electron spectrum is constant at depths greater than the depth of the dose maximum d_{max}. Ionization measurements are made with a fixed source–detector distance at depths of 10 and 20 cm. The ratio of the 20-cm reading to the 10-cm reading is related to water/air, polystyrene/air, and acrylic/air stopping-power ratios in Fig. 2. In the figure, the ionization ratio is also related to the "nominal accelerating potential" of the x-ray source. This new parameter, the nominal accelerating potential, is introduced mainly as a matter of convenience and to retain a commonly used nomenclature. Few physicists or radiotherapists would want to describe their accelerators in terms of the ionization ratio, and it is reasonable to describe x-ray quality in units of megavolts. It should be kept in mind that the ionization ratio and nominal accelerating potential are similar to the half-value layer concept; they afford the best means presently available for selecting the appropriate stopping-power ratio but they do not uniquely define the photon spectrum or the true accelerating potential.

For electron beams, the incident spectrum is constantly degraded with depth of penetration. The stopping-power ratios given in Sec. IV B were calculated for broad beams of monoenergetic electrons incident upon a semi-infinite phantom. The depth of the 50% dose level for these monoenergetic electrons is related to their incident energy by the factor 2.33 MeV/cm. To be consistent with the calculated depth-dose and stopping-power data, it is recommended that the mean incident energy of the user's beam be determined by multiplying the depth of the 50% dose on the central axis by 2.33 MeV/cm. The appropriate stopping-power ratio is obtained from Tables V–VII by matching the user's phantom material, calibration depth, and mean incident energy with the corresponding parameters in the tables.

C. Dosimeters

The primary method of dosimetry recommended by the Protocol requires an ionization chamber having a calibration factor for ^{60}Co gamma rays *directly traceable*[†] to NBS. The use of a national standard to characterize the response of an ionization chamber assures both accurate and consistent therapy machine calibrations. For ionization chambers intended for use with a specific electrometer, the exposure-calibration factor will have the units of roentgens per scale

[†] "Directly traceable" means that the instrument has either been calibrated at NBS, or has been calibrated at an ADCL against a secondary standard that has itself been calibrated at NBS (Ref. 51).

division; for chambers having electrical connectors that permit their connection to a variety of calibrated electrometers, the comparable units will be roentgens per coulomb. As the accuracy of most charge-measuring electrometers depends upon the stability of a capacitor in the feedback loop of an amplifier, it is as important to routinely calibrate the electrometer (coulombs/scale division) as it is to calibrate the ionization chamber to which it is connected. Exposure-calibration factors, and therefore N_{gas} also, are referenced to the chamber response at 22 °C and one standard atmosphere pressure (760 mmHg), and care must be exercised in the application of the appropriate temperature and pressure corrections.

Although instruments of any reasonable dimensions can be calibrated in terms of exposure, this Protocol sets upper limits on the dimensions of the air cavity. For a cylindrical chamber placed with its axis perpendicular to the beam direction, the internal diameter should be no greater than 1 cm. Its internal height should be such that the radiation fluence is uniform from end to end for the smallest field size.

The uncertainty in the determination of dose to the dosimetry phantom will be less when the chamber composition is the same as the phantom, e.g., a polystyrene chamber in a polystyrene phantom. This is noticeably important for the dosimetry of electrons in the range of 5–15 MeV when using a plane-parallel chamber that has its collecting volume supported by a centimeter or more of solid plastic. Electrons that are backscattered from this plastic support make a significant contribution to the total ionization. As electron backscatter is a direct function of atomic number,[56] differences in the composition of the plastic support and the dosimetry phantom can cause the ionization to be higher or lower than would be obtained if the compositions were the same. For example, the response of a plane-parallel chamber that has a 1-cm-thick acrylic support, to 7-MeV electrons at d_{max} in water is about 1.5% less than would be obtained from the same chamber backed by only water.[49]

As for chamber geometry, chambers of the guarded field, plane-parallel design, typically having electrode spacings and diameters on the order of 2 mm and 2 cm, respectively, require smaller replacement corrections than cylindrical chambers, and their depths are accurately defined at the inner surface of the proximal collecting plate. Replacement corrections for cylindrical chambers in photon beams do not exceed 1.5%, and are less than 0.8% for Farmer-type chambers, however, for low-energy electron beams they can be as large as 4% for Farmer-type chambers and can exceed 5% for chambers with internal diameters greater than 7 mm. Available data indicate that the effective point of measurement for cylindrical chambers in electron beams is between two-thirds and three-quarters the inner radius in front of the chamber's axis. For the cylindrical chambers that meet the requirements of this Protocol, the uncertainty in the measurement depth at d_{max} for electron beams is less than 0.5 mm. Because the uncertainty in the determination of any physical parameter is reduced as the magnitudes of correction factors are reduced, plane-parallel chambers are preferable to cylindrical chambers when used in the same dosimetry phantom. This preference will be diminished when, for example, a plane-parallel chamber in a polystyrene phantom is compared with a cylindrical chamber in a water phantom, both irradiated with low-energy electrons. The uncertainties are minimized when a plane-parallel chamber is used in water, and are greatest when a cylindrical chamber is used in plastic. In accord with a supplement to the NACP protocol[57] plane-parallel chambers are preferred for electron-beam dosimetry in the range of 5–10 MeV.

Exposure calibration factors N_X for ^{60}Co gamma rays are at present provided in the United States by NBS, and by the AAPM ADCLs. The ADCLs are referenced to NBS by reference-class ionization chambers, and intercomparisons between the ADCLs and NBS take place at approximately yearly intervals. For the purposes of this Protocol, the calibrations provided by ADCLs are equivalent to those provided by NBS.

D. Buildup caps

For an ionization chamber to be suitable for in-air calibration in terms of exposure, the chamber wall must be thick enough to provide electron equilibrium at the sensitive volume. For orthovoltage x rays, wall thicknesses of 0.5 mm are more than adequate to satisfy this requirement, however, for ^{60}Co gamma rays, wall thicknesses of about 5 mm are required, and many chambers must be fitted with buildup caps. If such a chamber is used to measure exposure in a phantom, the buildup cap must be in place, and the exposure so determined is at the center of the cavity left in the phantom after the chamber with buildup cap is removed. For ^{60}Co gamma rays, it is questionable whether the in-air exposure-calibration factor is applicable to in-phantom measurements of exposure because of the presence of lower energy scattered photons that were not present in the calibration beam. In-phantom measurement of exposure plays no role in the dosimetric methods developed in this Protocol.

In the present Protocol, the ionization chamber approximates a gas-filled Bragg–Gray cavity in a solid or liquid extended medium. Under ideal conditions all of the ionization of the gas in the cavity is due to electrons that arise in the phantom material, and the dose to phantom is related to the dose to gas by the ratio of their average stopping powers. Experimental conditions come closer to the ideal when the chamber wall is of the same composition as the phantom, e.g., an acrylic chamber in an acrylic phantom. If the chamber wall and phantom are of different compositions, then some of the ionization will be due to electrons that arise in a material different from the phantom, and corrections will be required. Except when the buildup cap and phantom are of the same composition, the buildup cap should be removed so as to reduce the magnitude of the corrections. When water phantoms are used, and the chamber must be made waterproof, a thin, low-atomic-number sheath should be used, the electrons from which contribute less than 25% of the ionization in the chamber (see Sec. IV F).

E. Dosimetry phantoms

For uniformity in the calibration reports for radiation-therapy machines, the Protocol recommends that the dose per unit time or monitor unit be expressed in terms of the dose to water. The ionization measurements upon which the

calibration is based may, however, be made in polystyrene or acrylic[‡] plastics as well as in water. When plastic phantoms are employed, the irradiation geometry must be altered so that the dosimeter is exposed to the same photon fluence as that in a water phantom. The extent to which the irradiation geometry is altered depends upon the density of the plastic, and it is the responsibility of the medical physicist to determine the density of plastic dosimetry phantoms, or to select a responsible manufacturer who calibrates the thickness of each plastic slab and calibration depth in terms of mass per unit area. When plastic phantoms are used, the first step in the dosimetric calculations is to determine the dose to the plastic, and the second step is to transfer that dose to the dose to water.

F. Absorbed-dose calibrations

NBS also provides absorbed-dose calibrations for ^{60}Co gamma rays. A graphite calorimeter[11] positioned in a graphite phantom is used to establish the dose to graphite. Next, a thick-walled graphite ionization chamber is placed in a similar graphite phantom at the same depth as the core of the calorimeter. Under these conditions, the chamber is exposed to the same photon fluence as the calorimeter, and it may be calibrated in terms of dose to graphite. The ion chamber is then transferred to a water phantom where the source–chamber distance and the depth are scaled from those used with the graphite phantom so that the photon spectrum at the measurement point in the water is the same as the spectrum in graphite.[50] The response of the graphite chamber in water, when multiplied by the ratio of mass energy-absorption coefficients of water to graphite and a chamber replacement factor, yields the dose to water. The user's chamber is placed at the same depth in the water phantom as the graphite chamber, and an absorbed-dose calibration obtained from its response. Similar to exposure calibration factors, absorbed-dose calibration factors are expressed in terms of dose to water per scale division or dose per unit charge at the position of the center of the chamber in the absence of the chamber, i.e., when the chamber no longer perturbs the radiation field in water. The use of ^{60}Co absorbed-dose-calibrated chambers in the Protocol is described in Sec. III H.

G. Alternate methods

The user is urged to compare whenever possible the results obtained with this Protocol to those obtained by other, independent methods. Of specific interest are calorimeters and the Fricke ferrous-sulfate dosimeter because stopping-power ratios of the phantom material to a solid or liquid dosimeter are less sensitive to changes in electron spectra than are the stopping-power ratios of phantom materials to air, replacement corrections for a solid or liquid dosimeter are smaller than for an air-filled dosimeter, and the response of both of these dosimeters is independent of dose rate.

III. THE CAVITY-GAS CALIBRATION FACTOR N_{gas}

The mathematical conversion from ionization in a small, gas-filled cavity to energy absorbed in the material surrounding the cavity is based upon the well-known Bragg–Gray theory.[12] As applied to ionization chambers, the Bragg–Gray theory is essentially a two-step process: the first step requires that the dose to the gas in the cavity be determined, and the second step transfers the dose to gas to the dose to medium. Direct application of this theory requires that the volume of the ionization chamber be known with an uncertainty considerably smaller than the maximum acceptable uncertainty in dose to the absorbing medium. As the volume of the gas-filled cavity is difficult to determine for most ionization chambers in general use, a stratagem that relates the dose to the air in the chamber to the chamber exposure calibration factor has been developed, which is basically the same as that of the Nordic Association of Clinical Physicists (NACP).[22] This stratagem requires the use of various physical parameters, such as stopping-power ratios, which are subject to periodic revision as theory and calculational techniques are improved. In addition, perturbation of the radiation field by the ionization chamber, and its subsequent replacement by phantom material, present problems that require more thorough analysis by the medical physics community. These problems notwithstanding, the recommended approach to high-energy dosimetry is to regard exposure-calibrated ionization chambers in dosimetry phantoms as Bragg–Gray cavities. The various equations, physical data, and correction factors to convert the ionization chamber response to dose to the phantom material are presented below.

A. Relationship of the dose to the gas (air) in a chamber and the exposure calibration factor

Absorbed dose to the gas (air) in the cavity of an ionization chamber is related to the dose to the wall through the Bragg–Gray equation. Dose to the wall material can be related to dose to air in the absence of the chamber, which, in turn, is related to exposure, assuming electron equilibrium. Thus, dose to the gas in the cavity is related to the exposure calibration factor of an ionization chamber.

At NBS, exposure for ^{60}Co gamma rays was established from measurements made with a series of spherical, graphite ionization chambers of variable wall thickness.[14] Exposure is calculated from

$$X = \frac{1}{k} J_{gas} (\bar{L}/\rho)^{wall}_{gas} (\bar{\mu}_{en}/\rho)^{air}_{wall} (\beta_{wall})^{-1} \prod_i K_i, \quad (1)$$

where X is exposure (R); k is the charge produced in air per unit mass per unit exposure (2.58×10^{-4} C kg^{-1} R^{-1}); wall refers to the material of the ionization chamber, graphite; J_{gas} is the charge per unit mass of the gas (air) in the chamber (C/kg); $(\bar{L}/\rho)^{wall}_{gas}$ is the ratio of the mean, restricted, collision mass stopping power of the graphite wall material to that of the gas (air) in the chamber for the secondary electrons released by ^{60}Co gamma rays; $(\bar{\mu}_{en}/\rho)^{air}_{wall}$ is the ratio of the mean mass energy-absorption coefficient for air to that of the wall (graphite) for ^{60}Co gamma rays; β_{wall} is the quotient of absorbed dose by the collision fraction of kerma in the chamber wall, 1.005; $\prod_i K_i$ is a product of factors that account for water vapor content of the air, ionization recombination losses, stem scatter, correction to zero wall thickness, and some other small corrections.

The exposure calculated at NBS from Eq. (1) is that which is obtained at the position of the center of the graphite chamber when the chamber is removed and replaced by air.

[‡] Acrylic, as used in this protocol, means polymethylmethacrylate, which is commercially produced as Lucite, Plexiglas, and Perspex.

A calibration factor for the user's chamber is obtained by placing it at the same location as the NBS graphite chamber and giving it a known exposure. The exposure calibration factor for the user's chamber is given by

$$N_X = XM^{-1}, \tag{2}$$

where M is the electrometer reading for the dosimeter (C or scale division) normalized to 22 °C, a pressure of one standard atmosphere, and uncorrected for ionization recombination; N_X is the ^{60}Co exposure calibration factor (R/C or R/scale division).

For the range of x-ray and electron energies covered by this Protocol, the dose to the gas in the ionization chamber is directly related to the charge per unit mass in the gas by

$$D_{\text{gas}} = J_{\text{gas}}(W/e), \tag{3}$$

where D_{gas} is the dose to the gas (Gy) and W/e is the quotient of the average energy expended to produce an ion pair by the electronic charge. For room air, $W/e = 33.7$ J/C. For x-ray and electron beams in the energy range under consideration, W/e appears to be constant.[13] J_{gas} is assumed to be corrected for ion recombination.

As the response of the electrometer is also directly related to J_{gas}, the quotient of D_{gas} by the electrometer reading M is a constant which depends upon the dimensions and composition of the ionization chamber. Henceforth in this Protocol the ratio of D_{gas}/M will be referred to as the cavity-gas calibration factor N_{gas}, i.e.,

$$N_{\text{gas}} = D_{\text{gas}} A_{\text{ion}} M^{-1}, \tag{4}$$

where N_{gas} is the dose to the gas in the chamber per electrometer reading (Gy/C or Gy/scale division); A_{ion} is the ionization collection efficiency at the time of calibration at NBS or an ADCL.

By combining Eqs. (1)–(4) an expression for N_{gas} for the user's chamber is obtained. When the chamber wall and buildup cap are of the same material,

$$N_{\text{gas}} = N_X \frac{k(W/e)A_{\text{ion}} A_{\text{wall}} \beta_{\text{wall}}}{(\bar{L}/\rho)^{\text{wall}}_{\text{gas}}(\bar{\mu}_{\text{en}}/\rho)^{\text{air}}_{\text{wall}}}, \tag{5}$$

where A_{wall} is a factor that corrects for attenuation and scatter in the wall and buildup cap.

These factors are discussed in greater detail below. There are other chamber-specific phenomena, such as scatter from the supporting stem and radiation-induced electrical leakage, that affect N_{gas} but for which neither specific corrections nor correction rules are known. It is recommended that until appropriate data become available, these types of corrections be assigned a value of unity.

When the chamber wall and buildup cap are of different materials, N_{gas} is given by a semiempirical expression similar to the one given by Almond and Svensson[6]:

$$N_{\text{gas}} = N_X \times \frac{k(W/e)A_{\text{ion}} A_{\text{wall}} \beta_{\text{wall}}}{\alpha(\bar{L}/\rho)^{\text{wall}}_{\text{gas}}(\bar{\mu}_{\text{en}}/\rho)^{\text{air}}_{\text{wall}} + (1-\alpha)(\bar{L}/\rho)^{\text{cap}}_{\text{gas}}(\bar{\mu}_{\text{en}}/\rho)^{\text{air}}_{\text{cap}}}, \tag{6}$$

where α is the fraction of ionization due to electrons from the chamber wall, and $(1-\alpha)$ is the fraction of ionization due to electrons from the buildup cap.

The product $A_{\text{ion}} A_{\text{wall}}$ in Eqs. (5) and (6) is essentially the inverse of ΠK_i in Eq. (1). The reason for this change in nomenclature is to separate clearly the functions of Eqs. (1) and (5). Whereas Eq. (1) is used by NBS to standardize a ^{60}Co source in terms of exposure using graphite ionization chambers, and ΠK_i is generally greater than unity, Eqs. (5) and (6) are used to determine the cavity-gas calibration factor for the user's ionization chamber, and $A_{\text{ion}} A_{\text{wall}}$ will generally be less than unity.

There are several facets of N_{gas} which the reader should appreciate. N_{gas} is unique to each ionization chamber, is unaffected by the environment of the chamber, i.e., does not depend on the composition of the dosimetry phantom, and is applicable to all ionizing radiations for which W/e has the value quoted above. N_{gas} can be obtained from Eqs. (5) and (6) using any photon beam for which an exposure calibration factor can be obtained, and for which the other parameters are known with adequate accuracy. Because of the present widespread use of the ^{60}Co exposure calibration, and the accuracy with which the parameters of Eqs. (5) and (6) are known, it is recommended that N_{gas} be determined from N_X for ^{60}Co gamma rays.

It is planned that the ADCLs and NBS will provide both N_{gas} and N_X. When only N_X is provided, the user must know more about the construction and performance of the chamber than was previously required in order to calculate N_{gas}, and as far as possible the Protocol will provide information about commonly employed ionization chambers. In general, these will be cylindrical chambers having internal diameters of less than 1 cm, however, N_{gas} for plane-parallel chambers with plate separations of 2 mm or less may also be calculated from either Eqs. (5) or (6).

The user needs to calculate N_{gas} for the chamber only once, or whenever there is a change in the ^{60}Co exposure calibration factor N_X. In order to reduce the possibilities for errors in this calculation, it is recommended that Worksheet (1) in Sec. VIII be employed. The following sections deal with the individual parameters of Eqs. (5) and (6).

B. The exposure-calibration factor, N_X

The exposure-calibration factor N_X should be obtained from NBS or an ADCL. [Note that N_{gas} applies to the same temperature and pressure as N_X, and that corrections in the electrometer reading will have to be made when the chamber is used at temperatures or pressures that differ from 22 °C (295 K) and 760 mmHg.]

C. Ratios of stopping powers and mass energy-absorption coefficients for ^{60}Co gamma rays

Ratios of restricted, collision mass stopping powers, mass energy-absorption coefficients, and their products for some commonly employed chamber wall and buildup cap materials are listed in Table I.

D. Ion collection efficiency

The correction for ion collection efficiency A_{ion} applies to the in-air exposure calibration. As the exposure rates em-

TABLE I. Ratios of stopping powers (Ref. 15) and mass energy-absorption coefficients (Ref. 15) for ^{60}Co gamma rays.[a]

Chamber wall or buildup cap	$(\bar{L}/\rho)^{wall}_{air}(\Delta = 10$ keV)	$(\bar{\mu}_{en}/\rho)^{air}_{wall}$	Product
Polystyrene	1.112	0.928	1.032
Acrylic	1.103	0.925	1.020
Graphite	1.010	0.999	1.009
Tufnol			1.021[b]
Water	1.133	0.899	1.019
A-150	1.145	0.906	1.037
Nylon	1.141	0.910	1.038
C-552	1.000	1.000	1.000
Bakelite	1.080	0.945	1.021

[a] These data apply to ionization chambers exposed in air.
[b] Reference 16.

ployed for exposure calibrations are usually less than 100 R/min, the ion collection efficiencies for most of the commonly employed chambers, operating with collection potentials in the range of 180–360 V, will be greater than 0.995. There are, however, exceptions to this rule, and the reader is advised to consult with the laboratory at which his chamber was calibrated for guidance in the determination of the ion collection efficiency. For ionization chamber/electrometer systems that permit adjustment of the collecting potential, the reader is referred to Sec. IV C for a method for determining A_{ion}. The reader is cautioned that the exposure calibration factor N_X has not been corrected for ion collection efficiency by NBS or the ADCL. The direct application of the ion collection efficiency, which is a number less than unity, to Eqs. (5) and (6) is required in order to obtain a value of N_{gas} that is applicable to the chamber when all of the charge is collected. Subsequent application of the chamber to the determination of dose in the user's beam requires a correction for the ion collection efficiency that is appropriate to that situation.

E. Wall correction factor

The wall correction factor A_{wall} takes account of attenuation and scattering of the primary ^{60}Co beam in the wall and buildup cap of the ionization chamber. This correction relates the actual charge per unit mass of air in the chamber to that which would be produced if there were neither attenuation nor scatter in the wall and cap. Extensive calculations have been made by Nath and Schulz[18] to determine A_{wall} for a range of commonly used ionization chambers, and also to determine the effect of chamber volume and geometry as well as composition on A_{wall}. In general, the compositions of the chamber wall and buildup cap do not affect A_{wall} if the thickness is expressed in terms of mass per unit area, and the average atomic number is close to those of water or soft tissue. For example, A_{wall} for a graphite chamber with a graphite buildup cap will be the same as for the graphite chamber with an acrylic buildup cap if the radial thicknesses of each are the same in terms of mass per unit area. Table II lists some commonly used ionization chambers and their respective wall-correction factors. For ionization chamber designs different from those listed in Table II, the data in Table III may be used to calculate A_{wall}.

TABLE II. Wall correction factors A_{wall} for common ionization chambers (Ref. 18).

Chamber type	Inner diameter (cm)	Inner height (cm)	Wall plus cap thickness (g/cm^2)	A_{wall}
Capintec–Farmer 0.6 cm^3	0.75	2.38	0.67	0.990
Capintec 0.1 cm^3	0.40	0.55	0.55	0.991
PTW normal	0.50	1.80	0.42	0.994
PTW transit	0.90	2.30	0.45	0.994
PTW micro	0.35	1.20	0.57	0.988
Shonka 0.1 cm^3	0.45	1.15	0.60	0.989
Exradin T.E. (A-150)	0.90	0.85	0.59	0.983
Exradin A.E. (C-552)	0.90	0.85	1.07	0.973
Far West IC-18	0.46	1.15	0.64	0.989
Capintec plane parallel	1.60	0.24	0.573	0.995
Memorial Hospital parallel-plate model 30-404	2.54	0.20	0.500	1.008
Shonka 3 cm^3 (spherical)	1.84	...	1.18	0.962

F. Quotient of absorbed dose by collision fraction of kerma

The conceptual aspects of this parameter as well as its derivation and methods for determination have been presented by Loevinger.[19] It arises from the fact that the photon energy released at a point in the form of charged particles (kerma) is transported distally and on the average imparted to the medium at some distal point. Thus the absorbed dose is equal to the collision fraction of kerma at some proximal point, and at any given point the absorbed dose is greater than the collision fraction of kerma. In the calculation of N_{gas}, the parameter β is the quotient of the absorbed dose by the collision fraction of kerma in the wall of the ionization chamber.

TABLE III. Attenuation and scattering as a function of the internal dimensions of a cylindrical ionization chamber (Ref. 18). The tabulated data are the percentage attenuation and scattering (γ) per unit wall thickness (cm^2/g). The wall correction factor A_{wall} is calculated as shown in footnote a.

Inner axial length (cm)	Inner diameter (cm) 0.4	0.6	0.8	1.0
0.4	1.56	2.10	2.70	3.22
0.6	1.53	2.05	2.60	3.10
0.8	1.51	2.00	2.50	2.96
1.0	1.49	1.95	2.40	2.84
1.5	1.44	1.80	2.15	2.52
2.0	1.42	1.65	1.90	2.22
2.5	1.40	1.52	1.70	1.90

[a] $A_{wall} = 1 - (t\gamma/100)$ where the wall thickness t (g/cm^2) includes the chamber wall and buildup cap.

G. Fraction of ionization due to electrons from chamber wall

In order to calculate N_{gas} for a chamber having a buildup cap of composition different from the chamber wall, Eq. (6) requires the fraction of ionization due to electrons arising in the chamber wall α. Lempert *et al.*[20] have determined that α is independent of the compositions of the wall and buildup cap, as long as they are of low-atomic-number materials, and that α depends upon wall thickness specified in mass per unit area. A graph of α versus wall thickness for ^{60}Co gamma rays is shown in Fig. 1.

H. Absorbed-dose calibrated ionization chambers, N_D

As discussed in Sec. II, NBS can provide absorbed-dose calibrations for ^{60}Co gamma rays in water. Specifically, the absorbed-dose calibration factor N_D is defined by

$$N_D = D_{water}\, M^{-1}, \tag{7}$$

where D_{water} is the absorbed dose to water at the position of the chamber center with the chamber replaced by water (Gy), and M is the electrometer reading (C or scale divisions) uncorrected for ion recombination. The absorbed-dose calibration factor is related to the cavity-gas calibration factor by

$$N_{gas} = N_D \frac{A_{ion}\, A_{repl}}{(\bar{L}/\rho)^{wall}_{gas}(\bar{\mu}_{en}/\rho)^{water}_{wall}}, \tag{8}$$

where A_{repl} is a correction for replacement of water by the user's chamber at the time of the ^{60}Co absorbed dose calibration. Note that A_{repl} and A_{ion} are the reciprocals of P_{repl} and P_{ion} defined in Sec. IV A for the chamber in the user's beam.

As is the case for in-air exposure calibration, this expression is valid only when the chamber wall and buildup cap have a thickness equal to or greater than the range of the most energetic secondary electrons released by ^{60}Co gamma rays, and the wall and buildup cap are of the same composition. When the compositions of the chamber wall and buildup cap are different, an expression having the form of Eq. (6) must be employed. Since an absorbed-dose calibration is performed in phantom, the buildup cap may be just the phantom material.

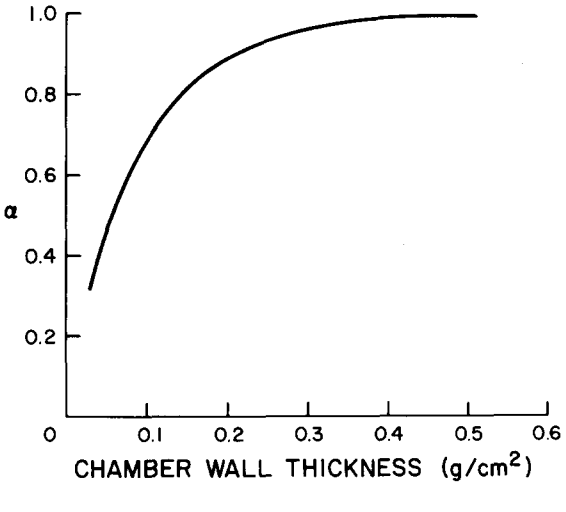

FIG. 1. The fraction of the ionization (α) due to electrons from the chamber wall irradiated by ^{60}Co gamma rays.

IV. DOSE TO THE MEDIUM

A. Spencer–Attix formulation of the Bragg–Gray relationship

Consider a gas-filled cavity in a medium that is irradiated by either a photon or an electron beam. Primary and secondary electrons[§] will enter and some will stop in the cavity, creating ionization there by inelastic collisions with the cavity gas. The well-known Bragg–Gray theory, in its simplest form, equates the ratio of the absorbed doses in the medium and the gas to the ratio of the mean unrestricted mass collision stopping powers[¶]:

$$D_{med}/D_{gas} = (\bar{S}/\rho)^{med}_{gas}.$$

There are several assumptions in this equation, the most important for present purposes being that the electron spectrum in the medium is not changed by the presence of the cavity, and the energy of a secondary electron is deposited at the position at which the electron is generated. The first assumption implies a cavity small in comparison with the ranges in the gas of the primary and secondary electrons, which is inconsistent with the second assumption, since an appreciable fraction of the secondary electrons generated in the cavity will have ranges in the gas that are large compared with the cavity size, and will dissipate some of their energy in the medium. Thus, some modification of the theory is required, and this modification must depend on the cavity size, in contrast to the original Bragg–Gray formulation, which is independent of cavity size.

While there is no fully rigorous theory of cavity ionization, the Spencer–Attix theory is widely used. In this theory, the secondary electrons are separated into two groups, divided at a cutoff energy Δ that corresponds approximately to the energy of an electron that can just cross the cavity. A "slow" secondary electron, with energy less than Δ, is considered to dissipate its energy at the point at which it is generated; a "fast" secondary electron, with energy greater than Δ, is counted as part of the electron slowing-down spectrum, and its energy is not considered to have been dissipated until it has dropped below Δ. Since the fast secondary electrons are accounted for in the slowing-down spectrum, their energies should not be included in the stopping power, which is now restricted to energy losses less than Δ. It is assumed that slow electrons released into the cavity from the chamber wall are in equilibrium with other slow electrons released from the gas that impinge upon the chamber wall, and there is no net energy transfer.

The Spencer–Attix formulation[12] can be expressed in the general form

$$D_{med}/D_{gas} = (\bar{L}/\rho)^{med}_{gas},$$

[§] Primary electrons include the electrons generated by photons in the case of a photon beam, and the incident electrons in the case of an electron beam. Secondary electrons are those generated by the primary electrons in the slowing down process, and include all subsequent generations of electrons.

[¶] Unrestricted stopping powers include all energy losses up to one-half the energy of the electron under consideration.

where $\bar{L}/\rho$ represents the restricted mean mass collision stopping power, averaged over the electron slowing-down spectrum in the wall material. In this equation, the electron slowing-down spectrum includes primary and secondary electrons with energies greater than Δ, and the restricted stopping powers include only energy losses less than Δ. These calculations include in the numerator and denominator of the ratio track-end corrections that account for secondary electrons that undergo inelastic collisions in which both electrons fall below Δ in energy.

Whereas the Bragg–Gray formulation of cavity theory uses unrestricted stopping powers averaged over the slowing-down spectrum of only the primary electrons, the Spencer–Attix formulation uses restricted stopping powers averaged over the slowing-down spectrum of all generations of electrons. Whereas the Bragg–Gray formulation is independent of cavity size, the Spencer–Attix formulation takes account of the finite size of practical ionization chambers by choosing a suitable value of the cutoff energy Δ. It has been shown that the restricted stopping-power ratio changes only slowly with the value of Δ. Practical ionization chambers, however, perturb the photon and electron fluence in various ways that must be accounted for by certain correction factors. Thus, a general relationship between dose to gas in the chamber and dose to medium that replaces the chamber when it is removed is given by

$$D_{\text{med}} = M N_{\text{gas}} (\bar{L}/\rho)^{\text{med}}_{\text{gas}} P_{\text{ion}} P_{\text{repl}} P_{\text{wall}}, \tag{9}$$

where M is the electrometer reading (C or scale divisions). When the chamber bias potential can be reversed, M should be the average of readings obtained with positive and negative potentials. med refers to the phantom material. $(\bar{L}/\rho)^{\text{med}}_{\text{gas}}$ is the ratio of the mean, restricted collision mass stopping power of the phantom material to that of the chamber gas (air). P_{ion} is a factor that corrects for ionization recombination losses that occur at the time of calibration of the user's radiation therapy beam; P_{ion} is the inverse of the ionization collection efficiency, and has a value equal to or greater than unity. P_{repl} is a replacement correction which depends upon the type and energy of the radiation, the gradient of the depth-dose curve at the point at which the measurement is made, and the radius of the chamber's air cavity. P_{wall} is unity when the chamber wall and the dosimetry phantom are of the same composition, is unity for electron beams, or is equal to

$$\frac{[\alpha(\bar{L}/\rho)^{\text{wall}}_{\text{gas}}(\bar{\mu}_{\text{en}}/\rho)^{\text{med}}_{\text{wall}} + (1-\alpha)(\bar{L}/\rho)^{\text{med}}_{\text{gas}}]}{(\bar{L}/\rho)^{\text{med}}_{\text{gas}}} \tag{10}$$

for photon beams when the chamber wall is of a composition different from the dosimetry phantom. α is the fraction of the total ionization produced by electrons arising in the chamber wall; $(1-\alpha)$ is the fraction of the total ionization produced by electrons arising in the dosimetry phantom; $(\bar{\mu}_{\text{en}}/\rho)^{\text{med}}_{\text{wall}}$ is the ratio of the mean mass energy-absorption coefficient for the dosimetry phantom (med) to that of the chamber wall, for the user's photon beam.

The rationale for P_{wall} equal to unity for electron beams is based upon the work of Johansson *et al.*[21] which shows that the response of relatively thin-walled ionization chambers composed of low-atomic-number materials is not affected by the wall composition. At this time, there are no data available which show how the response to electron beams of thick-walled chambers, or chambers having large central electrodes, is affected by differences in their composition and that of the dosimetry phantom, and an equation analogous to Eq. (10) for electron dosimetry has not been formulated.

For x-ray dosimetry, the buildup cap should not be used for in-phantom measurements unless it is of the same composition as the phantom, or is of the same composition as the chamber wall. In either case, Eq. (10) must be evaluated, however, when the buildup cap is the same as the chamber wall, α will be larger and the uncertainty in the dose calibration somewhat reduced. If the chamber wall, buildup cap, and phantom are of different compositions, e.g., a graphite chamber with an acrylic cap in a water phantom, an equation similar to Eq. (10), which includes a term for the fraction of ionization produced by electrons arising in the cap, would be necessary for the dose calculation. This protocol does not address the last-named situation.

For electron-beam dosimetry, it is recommended that the buildup cap be removed so that the electron spectrum traversing the air-filled cavity of the chamber is minimally changed from that in the surrounding medium.

Waterproofing of ionization chambers may be accomplished with thin rubber sheaths, stretched to the extent that they have a negligible effect upon the chamber response.

B. Stopping-power ratios

The doses calculated from Eq. (9) are critically dependent upon the choice of the correct stopping-power ratio, and stopping-power ratios are, in turn, dependent upon the spectrum of photons or electrons incident upon the dosimetry phantom. It is common for manufacturers to specify beam energy at the vacuum window of the beam line, however, because of subsequent energy degradation in the vacuum window, flattening filter or scattering foil, and beam-defining device, the x-ray or electron spectrum from one accelerator may be considerably different from that of another operating at the same nominal energy. Because a change in spectral quality is reflected by a change in the depth-dose curve, it is convenient to relate in-phantom ionization measurements to the nominal accelerating potential of x-ray beams or the mean incident energy $\bar{E}_0$ of electron beams. Subsequently, these parameters are used to select the stopping-power ratio appropriate to the x-ray or electron beam under consideration.

1. X-ray beams

For x-ray beams, the nominal accelerating potential is related to the ratio of ionization measurements made with a constant source–detector distance and two different phantom thicknesses. Water, polystyrene, or acrylic phantoms may be used for this determination, and the following parameters should be used.

Source–detector distance—1 m or the source–axis distance

Field size at detector—10×10 cm^2

Depth in phantom—	Water	Polystyrene	Acrylic
First measurement	10 cm	9.9 cm	8.8 cm
Second measurement	20 cm	19.8 cm	17.6 cm

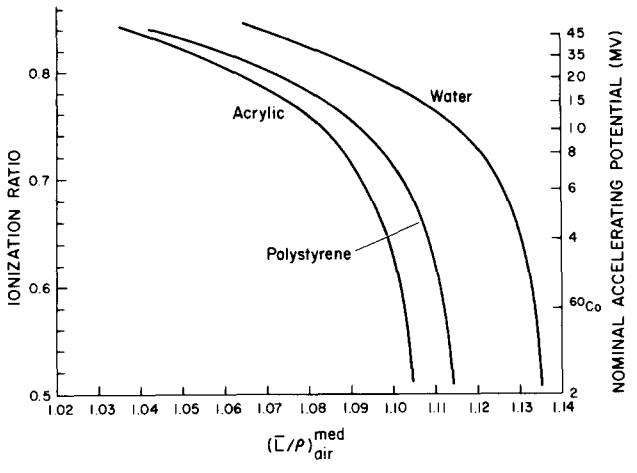

FIG. 2. Ratios of mean, restricted collision mass stopping powers of phantom materials to air $(\bar{L}/\rho)^{med}_{air}$ as a function of the ionization ratio and nominal accelerating potential.

The thicknesses of plastic are adjusted for differences in the electron concentration (e^-/cm^3) of the plastics relative to water (see Table X).

Experimentally determined ionization ratios, nominal accelerating potentials, and ratios of average stopping powers for water/air, polystyrene/air, and acrylic/air are related in the graphs shown in Figs. 2 and 3, which were obtained by an analysis made by Cunningham and Schulz.[25] Table IV lists average stopping-power ratios for a variety of chamber-wall materials versus nominal accelerating potential. These data are applicable only at or beyond d_{max}. In the buildup region, the mean energy of secondary electrons is higher, and $(\bar{L}/\rho)^{med}_{air}$ is lower than at d_{max}.

2. Electron beams

For electron beams, the mean incident energy is obtained by multiplying the depth in water at which an ionization-chamber reading is reduced to one-half of its maximum reading d_{50} by a numerical constant, 2.33 MeV/cm. This constant was obtained from an analysis of depth-dose curves calculated by Berger and Seltzer[45] for plane-parallel, infinitely wide beams of monoenergetic electrons incident upon a semi-infinite water phantom. In practice, d_{50} should be determined with a field size larger than that for which there is no increase in the depth of d_{50}. The mean incident energy thus established is applicable to field sizes smaller than that used for the d_{50} determination. A typical depth-ionization curve is shown in Fig. 6.

When polystyrene or acrylic phantoms are used for the determination of $\bar{E}_0$, d_{50} must be scaled so as to take account of the differences between these plastics and water. Loevinger, Karzmark, and Weissbluth[44] have determined scaling factors for polystyrene and acrylic relative to water that permit dose measurements made in plastic to be converted to corresponding depths in water. These scaling factors for polystyrene and acrylic are 0.965 and 1.11, respectively. When d_{50} in plastic is expressed in centimeters,

$$\bar{E}_0 = 2.33 \times d_{50} \times f, \tag{11}$$

where f is the scaling factor. If d_{50} in plastic is expressed in g/cm^2,

$$\bar{E}_0 = 2.33 \times d_{50} \times f/\rho, \tag{12}$$

where ρ is the density of the plastic in g/cm^3 (Sec. V A).

Ratios relative to air of average restricted collision mass stopping powers $(\bar{L}/\rho)$ for monoenergetic electron beams with incident energies in the range of 1–60 MeV are listed in Tables V–VII for water, polystyrene, and acrylic. Because the incident, monoenergetic spectrum is degraded as it penetrates into the phantom, $(\bar{L}/\rho)^{med}_{air}$ increases significantly with depth, and it is important to measure the depth accurately even for measurements made in the region of d_{max}. These ratios were calculated by Berger[23] for an infinitely wide, plane-parallel beam of electrons incident upon a semi-infinite phantom, however, they may be used for the range of field sizes commonly employed in radiation therapy. As for the photon-beam stopping powers, a cutoff energy of 10 keV was employed. The stopping-power ratio appropriate to the user's beam is selected by using the mean incident energy $\bar{E}_0$ as the electron beam energy in the Berger tables.

C. Ionization recombination correction

If all of the charge in the ionization chamber is not collected, the dose calculated from Eq. (9) will be too small. Therefore, a correction is required for ions that recombine, and this correction is the inverse of the ionization collection efficiency. The collection efficiency of an ionization chamber is the ratio of the ionization current obtained under a specific set of measuring conditions, e.g., bias potential and dose rate, to the ionization current that would result from the collection of all ions formed in the sensitive volume of the chamber. The theory of ionization chamber collection efficiency for both pulsed and continuous radiation fields has been described by Boag.[24] Because of differences between the idealized geometries dealt with in theory and the more complex geometries of practical ionization chambers, it is

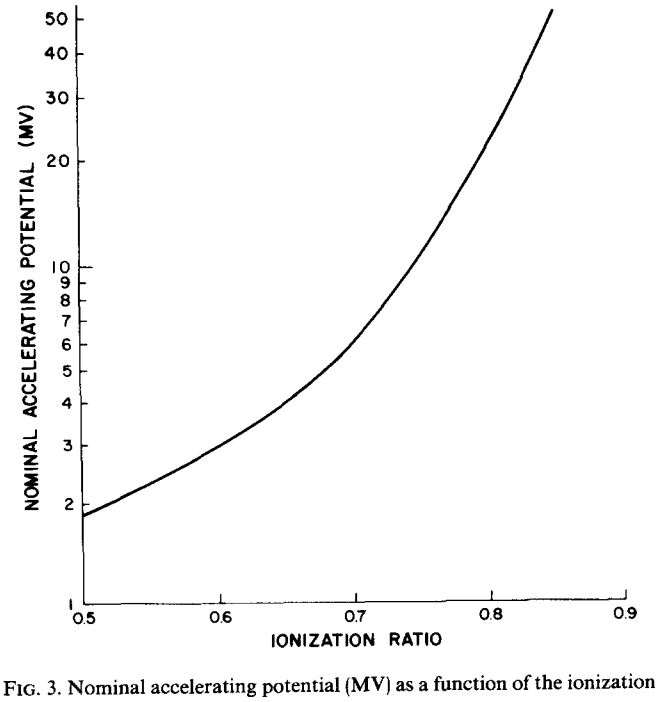

FIG. 3. Nominal accelerating potential (MV) as a function of the ionization ratio.

TABLE IV. Ratios of average, restricted stopping powers for photon spectra, $\Delta = 10$ keV (Ref. 25).

Nominal accelerating potential (MV)	$(\bar{L}/\rho)^{med}_{air}$							
	Water	Polystyrene	Acrylic	Graphite	A-150	C-552	Bakelite	Nylon
2	1.135	1.114	1.104	1.015	1.154	1.003	1.084	1.146
^{60}Co	1.134	1.113	1.103	1.012	1.151	1.000	1.081	1.142
4	1.131	1.108	1.099	1.007	1.146	0.996	1.075	1.136
6	1.127	1.103	1.093	1.002	1.141	0.992	1.070	1.129
8	1.121	1.097	1.088	0.995	1.135	0.987	1.063	1.120
10	1.117	1.094	1.085	0.992	1.130	0.983	1.060	1.114
15	1.106	1.083	1.074	0.982	1.119	0.972	1.051	1.097
20	1.096	1.074	1.065	0.977	1.109	0.963	1.042	1.087
25	1.093	1.071	1.062	0.968	1.106	0.960	1.038	1.084
35	1.084	1.062	1.053	0.958	1.098	0.952	1.027	1.074
45	1.071	1.048	1.041	0.939	1.087	0.942	1.006	1.061

recommended that the user of this Protocol experimentally determine the ionization collection efficiency of his chamber under the conditions that exist at the time of calibration of the therapy beam.

A convenient method for determining the ionization recombination correction P_{ion} is to make two sets of measurements, one with the normal bias potential applied to the chamber, and the other with the bias potential reduced by one-half. For this case, Boag[37] and Almond[35] have shown that the ratio of the charges collected can be related to P_{ion}. In Fig. 4, the three curves apply to continuous radiation as produced by ^{60}Co, pulsed radiation as produced by accelerators that use flattening filters or scattering foils to obtain large field sizes, and scanning, pulsed beams as produced by some accelerators as an alternate method for obtaining large fields. It is recommended that the normal bias potential be increased when the collection efficiency is less than 0.95.

D. Replacement correction

In the process of determining the dose to a solid or liquid medium from the ionization in a gas-filled cavity inserted into that medium, various phenomena occur which cause the electron fluence in the cavity to differ from the fluence in the medium which replaces the cavity after it is removed. Unless corrections are applied, this difference in electron fluence will generally result in an overestimation of the dose to the medium. There are two major components to what are referred to in this Protocol as replacement corrections: gradient corrections and electron fluence corrections.

1. Gradient corrections

Gradient corrections are required whenever the ionization chamber is at a location where the dose gradient has a nonzero slope, e.g., on the descending portion of the depth-dose curve, and the magnitude of the correction increases with the slope as well as with the inner radius of the chamber. Gradient corrections are required in general for both x-ray and electron dosimetry, however, it is recommended that electron-beam dose calibrations be done only with the chamber at d_{max} where gradient corrections are not required.

Gradient corrections arise because, in this Protocol, the central axis of a cylindrical ionization chamber positioned perpendicular to the radiation beam is taken as the measurement depth. It is at this depth that the dose to the phantom is to be determined. On the descending portion of a depth-dose curve, the fluence of secondary electrons is decreasing, and the proximal surface of a cylindrical cavity intercepts an electron fluence that is more intense than that at the measurement depth when the chamber is removed. Gradient corrections for cylindrical chambers as a function of x-ray beam energy and internal diameter are given in Fig. 5. These data were derived from those published by Cunningham and Sontag,[26] and are applicable to measurements made on the descending, approximately exponential, portion of the central-axis depth-dose curve. Gradient corrections are not required for plane-parallel chambers where the depth of measurement is taken at the inner surface of the proximal electrode.

An alternative to gradient corrections has been suggested by several investigators,[27–29] which is to regard the effective location of the ionization chamber to be at some point proximal to its central axis, e.g., at three-quarters of its internal radius for electron beams. This protocol does not use this approach because it does not take into account changes of the dose gradient, and because of the likelihood of errors being made in the specification of the calibration depth.

The gradient correction is unrelated to the factor A_{eq}, which accounts for attenuation and scatter in a small mass of tissue exposed in free air to x rays or gamma rays, and it bears only a tenuous relationship to what has been called a displacement factor, A_c, which is restricted to ^{60}Co gamma rays. For a detailed discussion of A_{eq} and A_c, the reader is referred to Johns and Cunningham.[30]

2. Electron fluence corrections

It is generally accepted that corrections for perturbation of the electron fluence are required whenever the ionization chamber is at a location where charged-particle equilibrium has not been established, i.e., in the dose-buildup region of high-energy x-ray beams and at all points in electron-beam dose distributions. Electron fluence corrections are not required for x-ray dose determinations made at or beyond d_{max} because so-called transient electron equilibrium can be assumed to exist at these locations.

TABLE V. Water/air stopping-power ratio (Δ = 10 keV) (Ref. 23).

Depth	Electron beam energy (MeV)																			
g/cm^2	60.0	50.0	40.0	30.0	25.0	20.0	18.0	16.0	14.0	12.0	10.0	9.0	8.0	7.0	6.0	5.0	4.0	3.0	2.0	1.0
0.0	0.902	0.904	0.912	0.928	0.940	0.955	0.961	0.969	0.977	0.986	0.997	1.003	1.011	1.019	1.029	1.040	1.059	1.078	1.097	1.116
0.1	0.902	0.905	0.913	0.929	0.941	0.955	0.962	0.969	0.978	0.987	0.998	1.005	1.012	1.020	1.030	1.042	1.061	1.081	1.101	1.124
0.2	0.903	0.906	0.914	0.930	0.942	0.956	0.963	0.970	0.978	0.988	0.999	1.006	1.013	1.022	1.032	1.044	1.064	1.084	1.106	1.131
0.3	0.904	0.907	0.915	0.931	0.943	0.957	0.964	0.971	0.979	0.989	1.000	1.007	1.015	1.024	1.034	1.046	1.067	1.089	1.112	1.135
0.4	0.904	0.908	0.916	0.932	0.944	0.958	0.965	0.972	0.980	0.990	1.002	1.009	1.017	1.026	1.036	1.050	1.071	1.093	1.117	1.136
0.5	0.905	0.909	0.917	0.933	0.945	0.959	0.966	0.973	0.982	0.991	1.003	1.010	1.019	1.028	1.039	1.054	1.076	1.098	1.122	
0.6	0.906	0.909	0.918	0.934	0.946	0.960	0.967	0.974	0.983	0.993	1.005	1.012	1.021	1.031	1.043	1.058	1.080	1.103	1.126	
0.8	0.907	0.911	0.920	0.936	0.948	0.962	0.969	0.976	0.985	0.996	1.009	1.016	1.026	1.037	1.050	1.067	1.090	1.113	1.133	
1.0	0.908	0.913	0.922	0.938	0.950	0.964	0.971	0.979	0.988	0.999	1.013	1.021	1.031	1.043	1.058	1.076	1.099	1.121		
1.2	0.909	0.914	0.924	0.940	0.952	0.966	0.973	0.981	0.991	1.002	1.017	1.026	1.037	1.050	1.066	1.085	1.108	1.129		
1.4	0.910	0.916	0.925	0.942	0.954	0.968	0.976	0.984	0.994	1.006	1.022	1.032	1.044	1.058	1.075	1.095	1.117	1.133		
1.6	0.912	0.917	0.927	0.944	0.956	0.971	0.978	0.987	0.997	1.010	1.027	1.038	1.050	1.066	1.084	1.104	1.124			
1.8	0.913	0.918	0.929	0.945	0.957	0.973	0.981	0.990	1.001	1.014	1.032	1.044	1.057	1.074	1.093	1.112	1.130			
2.0	0.914	0.920	0.930	0.947	0.959	0.975	0.983	0.993	1.004	1.018	1.038	1.050	1.065	1.082	1.101	1.120	1.133			
2.5	0.917	0.923	0.934	0.952	0.964	0.981	0.990	1.000	1.013	1.030	1.053	1.067	1.083	1.102	1.120	1.131				
3.0	0.919	0.926	0.938	0.956	0.969	0.987	0.997	1.008	1.023	1.042	1.069	1.084	1.102	1.119	1.129					
3.5	0.922	0.929	0.941	0.960	0.974	0.994	1.004	1.017	1.034	1.056	1.085	1.102	1.118	1.128						
4.0	0.924	0.932	0.944	0.964	0.979	1.001	1.012	1.027	1.046	1.071	1.101	1.116	1.126							
4.5	0.927	0.935	0.948	0.969	0.985	1.008	1.021	1.037	1.059	1.086	1.115	1.125	1.127							
5.0	0.929	0.938	0.951	0.973	0.990	1.016	1.030	1.049	1.072	1.101	1.123	1.126								
5.5	0.931	0.940	0.954	0.978	0.996	1.024	1.040	1.061	1.086	1.113	1.125									
6.0	0.934	0.943	0.958	0.983	1.002	1.033	1.051	1.074	1.100	1.121										
7.0	0.938	0.948	0.965	0.993	1.017	1.054	1.075	1.099	1.118	1.122										
8.0	0.943	0.954	0.972	1.005	1.032	1.076	1.098	1.116	1.120											
9.0	0.947	0.960	0.981	1.018	1.049	1.098	1.114	1.118												
10.0	0.952	0.966	0.990	1.032	1.068	1.112	1.116													
12.0	0.962	0.980	1.009	1.062	1.103															
14.0	0.973	0.996	1.031	1.095	1.107															
16.0	0.986	1.013	1.056	1.103																
18.0	1.000	1.031	1.080																	
20.0	1.016	1.051	1.094																	
22.0	1.032	1.070																		
24.0	1.048	1.082																		
26.0	1.062	1.085																		
28.0	1.071																			
30.0	1.075																			

754

TABLE VI. Polystyrene/air stopping-power ratio ($\Delta = 10$ keV) (Ref. 23).

Depth	Electron beam energy (MeV)																		
g/cm^2	60.0	50.0	40.0	30.0	25.0	20.0	18.0	16.0	14.0	12.0	10.0	9.0	8.0	7.0	6.0	5.0	4.0	3.0	2.0	1.0
0.0	0.875	0.878	0.887	0.903	0.915	0.929	0.936	0.943	0.950	0.959	0.970	0.975	0.982	0.990	0.999	1.010	1.030	1.049	1.069	1.089
0.1	0.876	0.879	0.888	0.904	0.916	0.930	0.936	0.943	0.951	0.960	0.970	0.977	0.983	0.991	1.000	1.011	1.032	1.052	1.074	1.100
0.2	0.876	0.880	0.889	0.905	0.917	0.931	0.937	0.944	0.952	0.961	0.972	0.978	0.985	0.993	1.002	1.013	1.034	1.056	1.080	1.109
0.3	0.877	0.881	0.890	0.906	0.917	0.931	0.938	0.945	0.953	0.962	0.973	0.979	0.986	0.994	1.004	1.016	1.038	1.061	1.086	1.114
0.4	0.878	0.882	0.891	0.907	0.918	0.932	0.939	0.946	0.954	0.963	0.974	0.980	0.988	0.996	1.007	1.019	1.042	1.066	1.092	1.116
0.5	0.878	0.883	0.892	0.908	0.919	0.933	0.940	0.947	0.955	0.964	0.975	0.982	0.990	0.999	1.009	1.023	1.046	1.071	1.098	
0.6	0.879	0.883	0.893	0.909	0.920	0.934	0.941	0.948	0.956	0.965	0.977	0.984	0.992	1.001	1.012	1.027	1.051	1.076	1.103	
0.8	0.881	0.885	0.894	0.911	0.922	0.936	0.943	0.950	0.959	0.968	0.980	0.983	0.996	1.006	1.019	1.035	1.060	1.087	1.111	
1.0	0.882	0.887	0.896	0.912	0.924	0.938	0.945	0.952	0.961	0.971	0.984	0.992	1.001	1.012	1.026	1.044	1.070	1.096		
1.2	0.883	0.888	0.898	0.914	0.926	0.940	0.947	0.955	0.963	0.974	0.988	0.996	1.006	1.019	1.034	1.054	1.080	1.105		
1.4	0.884	0.889	0.900	0.916	0.927	0.942	0.949	0.957	0.966	0.978	0.992	1.001	1.012	1.026	1.043	1.064	1.089	1.111		
1.6	0.886	0.891	0.901	0.918	0.929	0.944	0.951	0.959	0.969	0.981	0.997	1.007	1.019	1.033	1.052	1.073	1.098			
1.8	0.887	0.892	0.903	0.919	0.931	0.946	0.954	0.962	0.972	0.985	1.002	1.012	1.025	1.041	1.060	1.083	1.106			
2.0	0.888	0.894	0.904	0.921	0.933	0.948	0.956	0.965	0.975	0.989	1.007	1.018	1.032	1.049	1.069	1.092	1.110			
2.5	0.891	0.897	0.908	0.925	0.937	0.954	0.962	0.972	0.984	0.999	1.020	1.034	1.050	1.070	1.091	1.108				
3.0	0.893	0.900	0.911	0.929	0.942	0.959	0.969	0.979	0.992	1.010	1.035	1.051	1.069	1.090	1.105					
3.5	0.896	0.903	0.914	0.933	0.947	0.965	0.975	0.987	1.002	1.023	1.051	1.069	1.088	1.103						
4.0	0.898	0.905	0.917	0.937	0.951	0.971	0.982	0.995	1.013	1.036	1.068	1.086	1.101							
4.5	0.900	0.908	0.920	0.941	0.956	0.978	0.990	1.005	1.024	1.051	1.085	1.099	1.105							
5.0	0.902	0.910	0.923	0.945	0.961	0.985	0.998	1.015	1.037	1.067	1.097	1.103								
5.5	0.904	0.913	0.927	0.949	0.966	0.992	1.008	1.026	1.051	1.081	1.102									
6.0	0.906	0.915	0.930	0.954	0.972	1.000	1.017	1.038	1.065	1.093										
7.0	0.910	0.920	0.936	0.963	0.984	1.018	1.040	1.063	1.089	1.100										
8.0	0.914	0.925	0.943	0.973	0.998	1.039	1.063	1.086	1.098											
9.0	0.918	0.930	0.950	0.985	1.013	1.061	1.084	1.095												
10.0	0.922	0.936	0.958	0.997	1.030	1.081	1.093													
12.0	0.931	0.949	0.976	1.024	1.067															
14.0	0.942	0.963	0.995	1.056	1.085															
16.0	0.953	0.978	1.016	1.078																
18.0	0.966	0.994	1.041																	
20.0	0.979	1.011	1.061																	
22.0	0.994	1.030																		
24.0	1.008	1.047																		
26.0	1.023	1.057																		
28.0	1.036																			
30.0	1.045																			

TABLE VII. Acrylic/air stopping-power ratio (Δ = 10 keV) (Ref. 23).

Depth	Electron beam energy (MeV)																			
g/cm^2	60.0	50.0	40.0	30.0	25.0	20.0	18.0	16.0	14.0	12.0	10.0	9.0	8.0	7.0	6.0	5.0	4.0	3.0	2.0	1.0
0.0	0.870	0.874	0.882	0.898	0.909	0.923	0.929	0.936	0.944	0.953	0.963	0.969	0.975	0.983	0.992	1.003	1.023	1.043	1.063	1.083
0.1	0.871	0.875	0.883	0.899	0.910	0.924	0.930	0.937	0.945	0.953	0.964	0.970	0.976	0.984	0.993	1.005	1.025	1.046	1.068	1.093
0.2	0.872	0.875	0.884	0.900	0.911	0.925	0.931	0.938	0.945	0.954	0.965	0.971	0.978	0.986	0.995	1.007	1.028	1.050	1.073	1.101
0.3	0.872	0.876	0.885	0.901	0.912	0.925	0.932	0.939	0.946	0.955	0.966	0.972	0.979	0.988	0.997	1.010	1.031	1.054	1.079	1.106
0.4	0.873	0.877	0.886	0.902	0.913	0.926	0.933	0.939	0.947	0.956	0.967	0.974	0.981	0.990	1.000	1.013	1.035	1.059	1.085	1.107
0.5	0.874	0.878	0.887	0.902	0.914	0.927	0.933	0.940	0.948	0.958	0.969	0.975	0.983	0.992	1.003	1.016	1.040	1.064	1.091	
0.6	0.875	0.879	0.888	0.903	0.915	0.928	0.934	0.941	0.949	0.959	0.970	0.977	0.985	0.994	1.006	1.020	1.044	1.069	1.095	
0.8	0.876	0.880	0.889	0.905	0.916	0.930	0.936	0.944	0.952	0.962	0.974	0.981	0.989	1.000	1.012	1.029	1.054	1.080	1.103	
1.0	0.877	0.882	0.891	0.907	0.918	0.932	0.938	0.946	0.954	0.964	0.977	0.985	0.994	1.006	1.020	1.038	1.064	1.089		
1.2	0.878	0.883	0.893	0.909	0.920	0.934	0.940	0.948	0.957	0.968	0.981	0.990	1.000	1.012	1.028	1.048	1.073	1.097		
1.4	0.880	0.885	0.894	0.910	0.922	0.936	0.943	0.951	0.960	0.971	0.986	0.995	1.006	1.020	1.037	1.057	1.083	1.103		
1.6	0.881	0.886	0.896	0.912	0.924	0.938	0.945	0.953	0.963	0.975	0.990	1.000	1.012	1.027	1.045	1.067	1.091			
1.8	0.882	0.887	0.897	0.914	0.926	0.940	0.947	0.956	0.966	0.978	0.995	1.006	1.019	1.035	1.054	1.076	1.098			
2.0	0.883	0.889	0.899	0.915	0.927	0.942	0.950	0.958	0.969	0.982	1.000	1.012	1.026	1.043	1.063	1.085	1.103			
2.5	0.886	0.892	0.902	0.919	0.932	0.948	0.956	0.965	0.977	0.992	1.014	1.028	1.044	1.063	1.085	1.101				
3.0	0.888	0.895	0.906	0.923	0.937	0.953	0.962	0.973	0.986	1.004	1.029	1.045	1.063	1.083	1.098					
3.5	0.891	0.898	0.909	0.927	0.941	0.959	0.968	0.980	0.996	1.016	1.045	1.063	1.082	1.096						
4.0	0.893	0.900	0.912	0.931	0.946	0.965	0.975	0.989	1.006	1.030	1.062	1.080	1.094							
4.5	0.895	0.903	0.915	0.935	0.951	0.971	0.983	0.998	1.018	1.045	1.079	1.092	1.097							
5.0	0.897	0.905	0.918	0.939	0.956	0.978	0.991	1.008	1.031	1.061	1.090	1.096								
5.5	0.900	0.908	0.921	0.943	0.962	0.986	1.000	1.020	1.045	1.075	1.095									
6.0	0.902	0.910	0.924	0.947	0.968	0.994	1.010	1.032	1.059	1.086										
7.0	0.905	0.915	0.930	0.957	0.981	1.012	1.033	1.058	1.083	1.092										
8.0	0.909	0.920	0.937	0.967	0.995	1.033	1.056	1.080	1.090											
9.0	0.913	0.925	0.945	0.979	1.011	1.055	1.077	1.088												
10.0	0.917	0.931	0.953	0.991	1.029	1.075	1.086													
12.0	0.926	0.943	0.970	1.018	1.067															
14.0	0.937	0.957	0.989	1.051	1.076															
16.0	0.948	0.973	1.011	1.071																
18.0	0.961	0.989	1.036																	
20.0	0.974	1.006	1.055																	
22.0	0.989	1.025																		
24.0	1.004	1.042																		
26.0	1.019	1.050																		
28.0	1.031																			
30.0	1.039																			

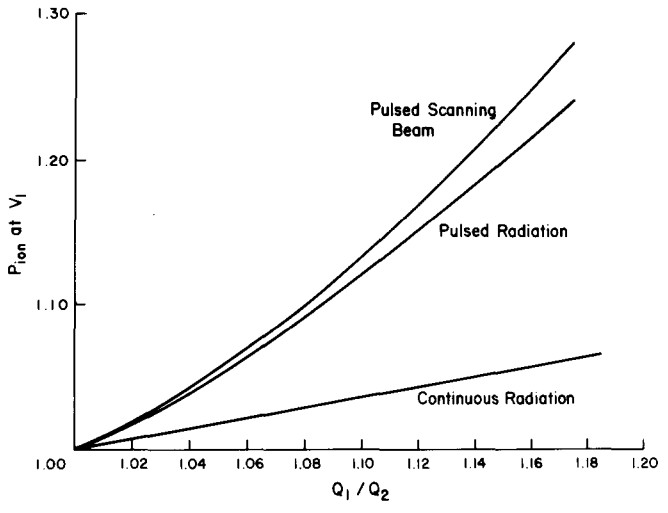

FIG. 4. Ionization recombination correction factors (P_{ion}) for continuous radiation (^{60}Co, Van de Graaff), pulsed radiation (accelerator-produced x rays and electron beams broadened by scattering foils), and pulsed scanning beams (magnetically scanned electron beams). These data are only applicable when $V_1 = 2V_2$.

Fluence corrections for electron beams were originally described by Harder,[31] and subsequently by Svensson and Brahme.[32] The number of electrons and the overall track length of electrons in the gas-filled cavity of an ionization chamber are, in general, different from those in a comparable volume of phantom material. The number of electrons entering the cavity is enhanced because more electrons are scattered in from adjacent phantom material than are scattered out by the gas. This results in a dose to the gas that is greater than that which would be produced by the unperturbed electron fluence in the phantom material. At the same time, the overall track length of electrons traversing the cavity is less than in a comparable volume of phantom material because electrons undergo fewer scattering interactions and their tracks in the gas are straighter. This results in a dose to the gas that is less than that produced by the same electron fluence in the phantom material. These two effects, generally referred to as in-scattering and obliquity, depend upon the dimensions and geometry of the ionization chamber.

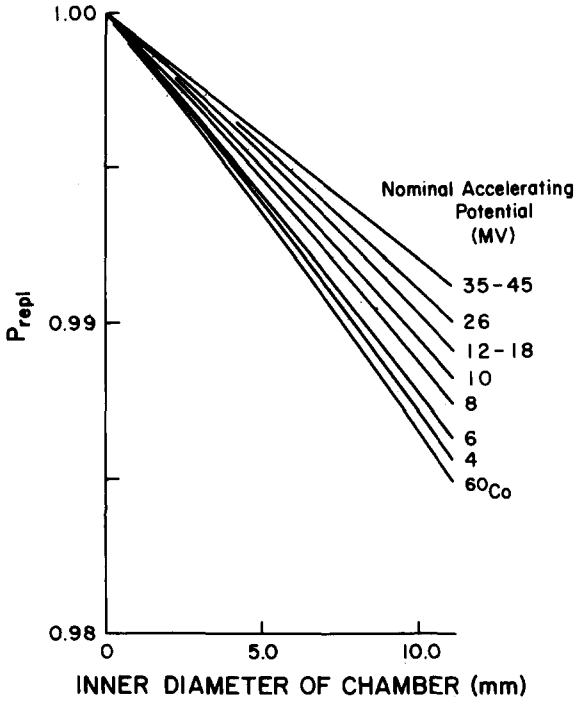

FIG. 5. Gradient corrections (P_{repl}) for photon beams as a function of the inner diameter of a cylindrical chamber and the nominal accelerating potential of the accelerator. Gradient corrections are not required for measurements made at d_{max}.

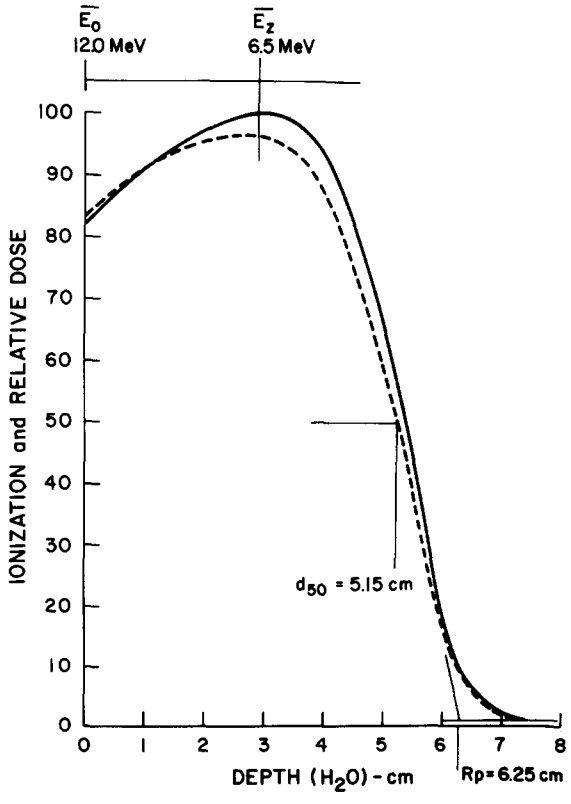

FIG. 6. Depth-ionization (dashed) and depth-dose (solid) curves for an electron beam. The mean incident energy ($\bar{E}_0$) is obtained from d_{50} of the depth ionization curve. The mean energy at d_{max} ($\bar{E}_z$) is obtained from $\bar{E}_0$ and R_p. When cylindrical chambers are used to determine d_{50} and R_p, the point of measurement should be taken as proximal to the chamber axis by 0.75 of the chamber's internal radius.

Plane-parallel chambers, of the type described by Holt *et al.*,[17] having guarded fields and internal heights and diameters on the order of 2 mm and 2 cm, respectively, have the smallest corrections for in-scattering and obliquity, and the electron fluence correction for this type of chamber is taken as unity in this Protocol.

Cylindrical chambers that have internal diameters greater than a few millimeters exhibit the effects of in-scattering to a greater extent than obliquity, so that their readings must, in general, be reduced so as to obtain the correct dose to the phantom material. Johansson *et al.*[21] have compared the responses of a series of cylindrical ionization chambers with the response of a plane-parallel chamber exposed in acrylic plastic to electron beams. The electron fluence correction was found to increase as the inner diameter of the chamber was increased, and the mean energy of the electrons at the point of measurement decreased. Electron fluence corrections obtained from the Johansson paper are presented in Table VIII. Although these data are strictly applicable only

TABLE VIII. Electron fluence corrections for cylindrical chambers (Ref. 21).

$\bar{E}_z$[a] (MeV)	Inner diameter (mm) 3	5	6	7
2	0.977	0.962	0.956	0.949
3	0.978	0.966	0.959	0.952
5	0.982	0.971	0.965	0.960
7	0.986	0.977	0.972	0.967
10	0.990	0.985	0.981	0.978
15	0.995	0.992	0.991	0.990
20	0.997	0.996	0.995	0.995

[a] $\bar{E}_z$ is the mean electron energy at depth of measurement, and is given approximately by

$$\bar{E}_z = \bar{E}_0(1 - z/R_p),$$

where z is the depth of measurement and R_p is the practical range (see Fig. 6).

to acrylic phantoms, it is recommended that they be used for water and polystyrene until comparable data become available for these materials.

E. Ratios relative to air of mean mass energy-absorption coefficients

Ratios relative to air of mean mass energy-absorption coefficients for ^{60}Co and x-ray beams in the range of 2 to 50 MeV are listed in Table IX for a variety of materials pertinent to high-energy dosimetry. These ratios were calculated by Cunningham[15] for the photon spectra that correspond to the nominal accelerating potentials listed in Fig. 2 and Table IV. The ratio of the mean mass energy-absorption coefficient for the phantom material (med) to that of the chamber wall (wall) is required by Eq. (10) for the calculation of the dose to the phantom material when the wall of the ionization chamber has a composition different from the phantom. The required ratio can be obtained by dividing the phantom/air ratio by the chamber-wall/air ratio which yields the phantom/chamber-wall ratio.

F. Fraction of ionization due to electrons from the chamber wall

When the wall of the ionization chamber, without buildup cap, has a composition different from that of the dosimetry phantom, it is necessary [for use in Eq. (10)] to determine the fraction α of the ionization that is due to secondary electrons released from the chamber wall by the incident x-ray beam. For the range of chamber-wall and dosimetry phantom materials normally employed, it can be shown that large uncertainties in α have only a very small effect on the dose calculated from Eq. (9). Also, α is relatively insensitive to the composition of the chamber wall so that, for example, graphite and acrylic chambers, having the same wall thickness in mass per unit area, will have nearly the same α. Lempert *et al.*[20] have measured α for a range of wall thicknesses and x-ray energies, and recommended values are given in Fig. 7.

G. The ^{60}Co buildup cap and in-phantom measurements

With the exception of the ^{60}Co exposure calibration and the in-air calibration of ^{60}Co units, the ^{60}Co buildup cap plays no role in this Protocol, and it is recommended that the cap be removed from the chamber for in-phantom measurements except when the composition of the cap and the dosimetry phantom are the same. The practice of using the buildup cap to waterproof the chamber complicates the dose calculation by introducing a third component that, in addition to the chamber wall and medium, releases electrons that contribute to the ionization of the gas. Ionization chambers, which are not inherently waterproof, should be protected by a thin sheath having a composition and density close to those of water. Under these conditions, a 0.5-mm sheath will contribute less than 25% of the ionization, and its effect on the dose calculation will be negligible.

V. DOSIMETRY PHANTOMS

A. Materials and dimensions

As the purpose in calibrating a radiation-therapy accelerator is to permit the accurate delivery of prescribed doses of radiation to various body tissues, it can be argued *a priori* that the transfer of dose will be accomplished with the least uncertainty if the dosimetry phantom has an atomic composition and mass density similar to the tissues that are most commonly treated. In all dosimetry protocols, water is the recommended material for dosimetry phantoms, and the material to which the dose calibration is referenced. The

TABLE IX. Ratios of mean mass energy-absorption coefficients (Ref. 25).[a]

Nominal accelerating potential (MV)	$(\bar{\mu}_{en}/\rho)^{med}_{air}$ Water	Polystyrene	Acrylic	Graphite	A-150	C-552	Bakelite	Nylon
2	1.111	1.072	1.078	0.992	1.100	1.000	1.051	1.090
^{60}Co–6	1.111	1.072	1.078	0.997	1.099	1.000	1.055	1.092
8	1.109	1.068	1.075	0.997	1.092	0.998	1.052	1.090
10	1.108	1.066	1.072	0.995	1.089	0.997	1.049	1.087
15	1.105	1.053	1.063	0.986	1.078	0.995	1.039	1.075
20	1.094	1.038	1.051	0.975	1.065	0.992	1.027	1.061
25	1.092	1.032	1.047	0.971	1.060	0.991	1.022	1.055
35	1.085	1.016	1.034	0.960	1.044	0.989	1.009	1.039
45	1.074	0.980	1.009	0.937	1.010	0.983	0.982	1.000

[a] These data are applicable to ionization measurements made in phantom.

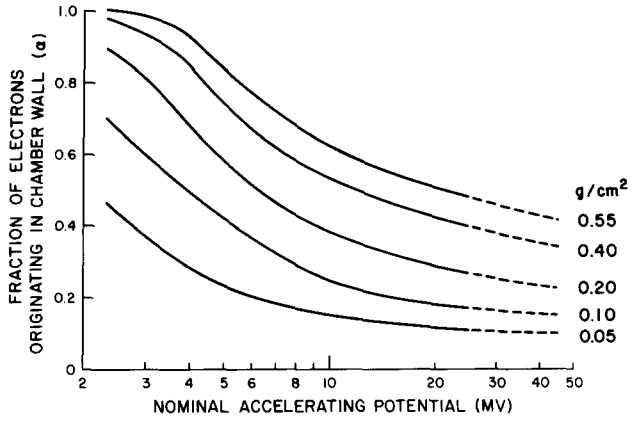

FIG. 7. Fraction of ionization (α) due to electrons from the chamber wall irradiated by x rays with nominal accelerating potentials of 2–50 MV. The dashed portions of the curves are extrapolations of experimental data (Ref. 20).

present protocol recommends that polystyrene and acrylic plastics, in addition to water, may be used for dosimetry phantoms, but, in agreement with other protocols, requires that the dose calibration be referenced to water.

Although many practical advantages are realized by the use of plastic dosimetry phantoms, these are partially offset by the need to modify the normally employed source–surface distance (SSD) for x-ray dosimetry, and to transfer the dose to plastic to the dose to water. The SSD modification is made (while the source–detector distance remains the same) so as to obtain the same attenuation of the incident x-ray beam in plastic as would be obtained if a water phantom were employed. Because the electron concentration in polystyrene is almost the same as in water, the same SSDs may be used with these phantoms with negligible error, however, as the electron concentration in acrylic is higher than that in water, small but significant SSD modifications are required when acrylic phantoms are used for x-ray dosimetry. The transfer of dose to plastic to dose to water for x rays is accomplished by application of the ratio of the average mass energy-absorption coefficient of water to that of plastic. As this parameter is accurately established and changes very slowly with beam energy, the dose transfer can be made with very little uncertainty. The transfer of dose to plastic to dose to water for electrons is accomplished by application of the ratio of the average unrestricted collision mass stopping power for water to that for plastic, and a correction factor that accounts for the difference in electron fluence at d_{max} in plastic compared with that at d_{max} in water. The ratios of unrestricted stopping powers for water to polystyrene or water to acrylic are essentially independent of electron energy so that this aspect of the dose transfer introduces very little uncertainty into the dose calibration. Corrections for differences in electron fluence at d_{max} in water and plastic are not well established at the time of writing, and the data provided in Sec. V D are uncertain to the extent of about 1%.

The question of constancy in the composition of the plastics has been addressed by Schulz and Nath,[33] and they concluded that the composition of the plastics is sufficiently constant so as to introduce negligible error when they are employed as high-energy dosimetry phantoms. Small variations in the mass density of acrylic and polystyrene plastics were noted, so that it is important that this parameter be experimentally determined. Some physical properties of water, polystyrene, and acrylic are listed in Table X, and, for comparison, the ICRU formulation for muscle.[34]

The dimensions of a dosimetry phantom should provide a 5-cm margin on all four sides of the largest field size to be employed, and a depth sufficient to provide maximum backscatter at the point at which the dose determination is made. For the x-ray and electron energies included in this Protocol, 10 cm of phantom material beyond the dosimeter are adequate.

B. Depth of calibration

For x rays, the calibration depth depends upon the inner diameter of the ionization chamber and the energy of the beam; specific recommendations are given in Table XI. When the depth of the dose maximum d_{max} varies with field size, a phenomenon observed for linear accelerators operating at 20–30 MeV, it is recommended that the calibration depth be on the exponentially decreasing portion of the depth-dose curve. Calibrations should not be made at depths where the gradient of the depth-dose curve is changing from zero (at d_{max}) to its maximum value because the gradient corrections, P_{repl}, have not been evaluated for this region (see Sec. IV D).

For electron beams, the calibration depth is restricted to d_{max} in both plastic and water phantoms. For cylindrical chambers held perpendicular to the incident beam, the center of the chamber should be positioned so that the proximal 180° segment of the inner surface of the chamber wall intercepts not less than the 99% level on the ascending portion of the depth-ionization curve. Plane-parallel chambers are positioned with the inner surface of the proximal electrode at d_{max}, and the dose so determined is at this depth. As the energy of an electron beam is reduced, the replacement factor P_{repl} for a cylindrical chamber increases as does the electron fluence correction ϕ_{med}^{water} that is required for the transfer of dose to plastic to dose to water. Thus, for electrons in the range of 5–10 MeV, particular care should be taken in the choice of dosimetry phantom and chamber to minimize the magnitude of these corrections, and thereby reduce the level of uncertainty in the dose determination. Plane-parallel chambers with a minimum amount of plastic construction to reduce electron backscatter, and water phantoms are nearly optimum in terms of this Protocol because neither gradient nor electron fluence corrections are required. Plane-parallel chambers in plastic phantoms require electron fluence corrections to obtain the dose to water, and cylindrical chambers in water require replacement corrections. Cylindrical chambers in plastic phantoms require both types of corrections, and this system should be avoided for electron-beam energies below 10 MeV.

C. Scaling factors and dose transfer, plastic to water (photons)

When the spectral distribution and fluence of primary and scattered photons at the measurement point in a plastic phantom are the same as at a comparable point in a water phantom, the dose to water is given by

TABLE X. Physical properties of water, acrylic, and polystyrene plastics, and muscle.

	Water	Acrylic	Polystyrene	ICRU muscle
Composition	H_2O	$C_5H_8O_2$	C_8H_8	
Density (g/cm^3)	1.00	1.17[a]	1.04[a]	1.00
Average atomic number $\bar{Z}$[b]	7.22	6.24	5.62	7.10
$\bar{Z}$ relative to water	1.000	0.86	0.78	0.98
Electron density (e$^-$/g)	3.346×10^{23}	3.253×10^{23}	3.243×10^{23}	3.32×10^{23}
Electron concentration (e$^-$/cm^3)	3.346×10^{23}	3.806×10^{23}	3.373×10^{23}	3.32×10^{23}
Electron concentration relative to water	1.000	1.137[a]	1.008[a]	0.992

[a] Nominal values; the mass density of each dosimetry phantom should be individually determined.
[b] The average atomic number $\bar{Z}$ is calculated by weighting the component atomic numbers by parts by weight.

$$D_{water} = D_{med}(\bar{\mu}_{en}/\rho)^{water}_{med}, \quad (13)$$

where D_{med} is given by Eq. (9) and $(\bar{\mu}_{en}/\rho)^{water}_{med}$ is the ratio of the average mass energy-absorption coefficient for water to that for plastic (Table XII).

Under ideal conditions (a point source of primary photons, only Compton interactions in the phantom, and a complete absence of photons scattered from the collimator or other components of the treatment head), the same spectral distribution is obtained in water and plastic when the source–surface distance (SSD) and dosimeter depths are scaled by the relative electron concentrations of plastic to water, and the collimator field size is not changed.[46,50,53] Under these conditions, the dose to water is related to the dose to plastic by

$$D_{water} = D_{med}(\bar{\mu}_{en}/\rho)^{water}_{med}(SDD^2)^{med}_{water}, \quad (14)$$

where $(SDD^2)^{med}_{water}$ is the ratio of the square of the source–detector distance for the plastic phantom to that for the water phantom.

Under practical conditions, collimators and other components of the treatment head contribute a significant number of scattered photons to the primary beam, and the inverse square law no longer provides an accurate description of fluence as a function of distance from the source. In addition, at photon energies greater than 25 MeV, the cross section for pair production exceeds that for the Compton interaction, and scaling based upon electron concentration is no longer applicable. For these reasons, it is recommended that the SDD and collimator field size for a plastic phantom be the same as for a water phantom, and that the overlying thickness of plastic be scaled so that the attenuation of the incident beam in plastic is equal to that in water.

Equal attenuation of the incident beam is obtained when the thickness of the plastic is related to the thickness of water by a scaling factor SF given by

$$SF = d_{plastic}/d_{water} = \bar{\mu}_{water}/\bar{\mu}_{plastic}, \quad (15)$$

where d is depth, and $\bar{\mu}$ is the mean linear attenuation coefficient, calculated for the incident photon spectrum.

Scaling factors for polystyrene and acrylic plastics for ^{60}Co gamma rays and x rays with nominal accelerating potentials in the range of 2 to 50 MV are listed in Table XIII. These factors are the ratios of linear plastic thickness to linear water thickness that result in equal x-ray attenuation.

When the SDD and collimator field size are the same for measurements made in water and plastic, approximately the same volume of phantom is irradiated in each case. Depending upon density and composition, the number of photons scattered by a plastic phantom will be different from the number scattered by a water phantom. Casson[46] has shown that the fractional increase in scattered photons, which occurs in polystyrene and acrylic phantoms, is equal to the ratio of the TAR for the unscaled field size to the TAR for the scaled field size:

$$\text{Excess scatter correction (ESC)} = \frac{TAR(F,d)}{TAR(Fc,d)}, \quad (16)$$

where F is the field size at depth d in water, and c is the relative electron concentration of plastic to water (Table X).

Table XIV lists excess scatter corrections for ^{60}Co and 2-, 4-, and 6-MV x rays. Data are provided only for acrylic phantoms because the electron concentration of polystyrene is nearly the same as that for water, and excess-scatter corrections are negligible.

A comparison of the calibration geometry of acrylic and water dosimetry phantoms is shown in Fig. 8. When the recommended geometry is employed, the dose to water is related to the dose to plastic by

$$D_{water} = D_{med}(\bar{\mu}_{en}/\rho)^{water}_{med}(ESC). \quad (17)$$

TABLE XI. Calibration depths for x-ray beams.

Dosemeter I.D. or plane air gap (mm)	Photon energy range (MeV)	Calibration depth in water[a]
Less than 2	^{60}Co–2	plane parallel: d_{max} or 5 cm cylindrical: 5 cm
	4–15	d_{max} or 5 cm
	16–25	d_{max} or 7 cm
	26–50	d_{max} or 10 cm
2–6.0	^{60}Co–15	5 cm
	16–25	d_{max} or 7 cm
	26–50	d_{max} or 10 cm
6.1–10	^{60}Co–15	5 cm
	16–30	7 cm
	31–50	d_{max} or 10 cm

[a] Measured from the surface of the phantom to the center of cylindrical or spherical chambers, or to the proximal inner electrode surface for a plane-parallel chamber. When plastic phantoms are employed, these depths are scaled in accordance with Sec. V C.

TABLE XII. Ratios of the mean mass energy-absorption coefficient for water to that for plastic (Ref. 15).

Nominal accelerating potential (MV)	$(\mu_{en}/\rho)^{water}_{med}$ Water/polystyrene[a]	Water/acrylic[a]
2–6, (^{60}Co)	1.036	1.031
8	1.038	1.032
10	1.039	1.033
15	1.049	1.040
20	1.054	1.041
25	1.058	1.043
35	1.068	1.049
45	1.096	1.064

[a] Derived from the data in Table IX.

TABLE XIV. Corrections for excess scatter from an acrylic phantom.

Energy (MV)	Depth (cm)	Field size at depth (cm^2) 5×5	10×10	20×20	30×30
^{60}Co	0.5	0.997	0.996	0.995	0.996
	5.0	0.986	0.987	0.989	0.991
2	0.4	0.998	0.994	0.997	
	5.0	0.984	0.982	0.989	
4	1.0	0.998	0.997	0.998	
	5.0	0.994	0.993	0.993	
6	1.5	0.999	0.998	0.998	
	5.0	0.994	0.994	0.996	

D. Scaling factors and dose transfer, plastic to water (electrons)

Methods and data for the determination of dose to plastic from electrons are given in Sec. IV, and in Sec. V B the recommendation is made that the calibration depth for electrons be restricted to d_{max}. If the spectral distribution and electron fluence at d_{max} in water and plastic are the same, the dose to water is related to the dose to plastic by

$$D_{water} = D_{med}(\bar{S}/\rho)^{water}_{med}, \quad (18)$$

where $(\bar{S}/\rho)^{water}_{med}$ is the ratio of the average unrestricted mass stopping power of water to that of plastic.

If the spectral distributions are the same but the electron fluences are different, the dose to water is related to the dose to plastic by

$$D_{water} = D_{med}(\bar{S}/\rho)^{water}_{med}\phi^{water}_{med}, \quad (19)$$

where ϕ^{water}_{med} is the ratio of the electron fluence at d_{max} in water to that at d_{max} in plastic.

As for the spectral distributions in water and plastic, calculations of $\bar{E}_z$ at d_{max} for depth-dose curves measured in water, polystyrene, and acrylic (Sec. IV D) yield values that are the same within the range of experimental uncertainty. As $\bar{E}_z$ may be taken as an index of beam quality, it is reasonable to assume that the spectral distributions are also the same. An examination of stopping-power data lends further support to this argument. Small differences between $\bar{E}_z$, and presumably between the spectral distributions, in water and plastic have a negligible effect upon $(\bar{S}/\rho)^{water}_{med}$; an 18% change in $\bar{E}_z$ is required to cause a 1% change in the stopping-power ratio.

The ratios of mean unrestricted collision mass stopping powers for water to polystyrene and water to acrylic are very nearly constant for electrons in the range 0.1–50 MeV, and recommended values are given in Table XV.

TABLE XIII. Scaling factors for photon beams (Ref. 38).

Nominal accelerating potential (MV)	Polystyrene/water	Acrylic/water
^{60}Co, 2–8	0.99	0.88
10–35	1.00	0.88
40–50	1.01	0.89

As for electron fluence, published reports[47,49,55] and data made available to Task Group 21 show that the response of an ionization chamber at d_{max} in water is greater than at d_{max} in polystyrene, and that the magnitude of the difference increases as the electron energy is decreased. A theoretical analysis by Hogstrom and Almond[48] suggests that the electron fluence at d_{max} is a function of the mass angular scattering power of the phantom material. As angular scattering power increases with mean atomic number and decreasing electron energy, the theory is consistent with the limited experimental data that is available.

At the time of writing, the argument for making fluence corrections when transferring the dose to polystyrene to the dose to water is sufficiently documented to warrant the inclusion of specific recommendations in this Protocol. When using a polystyrene phantom for the dosimetry of electrons having mean incident energies $\bar{E}_0$, in the range of 5–16 MeV,

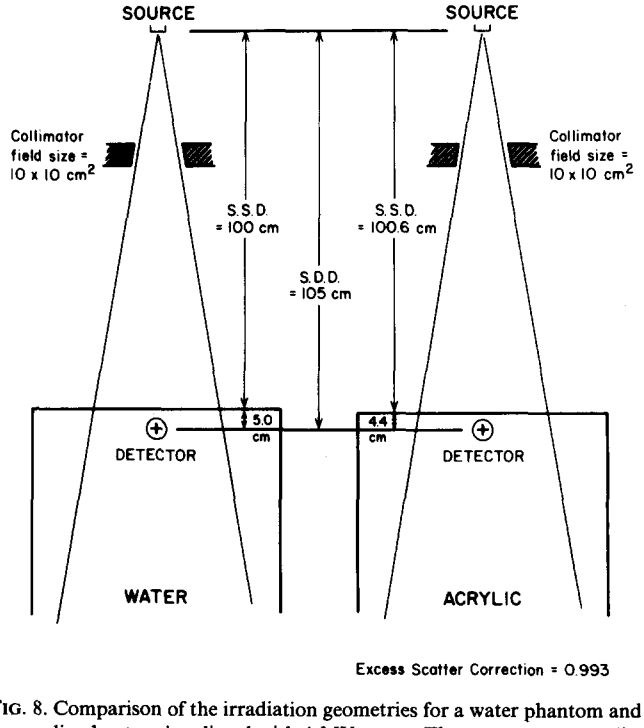

FIG. 8. Comparison of the irradiation geometries for a water phantom and an acrylic phantom irradiated with 4-MV x rays. The source–detector distance (SDD) and the collimator field size are the same for each phantom. The source–surface distance (SSD) is greater for the denser acrylic phantom, and a correction for excess scatter is also required.

TABLE XV. Ratios of unrestricted collision mass stopping powers (Ref. 36).

	Water/polystyrene	Water/acrylic
$(\bar{S}/\rho)^{\text{water}}_{\text{med}}$	1.030	1.033

the fluence corrections $\phi^{\text{water}}_{\text{med}}$ in Table XVI should be applied in the process of transferring the dose to water.

Although similar corrections should be made when acrylic phantoms are used, acrylic is for this purpose more nearly like water than polystyrene, and experiments have failed to show any significant differences of electron fluence in these two materials. Until data to the contrary are provided, it is recommended that a fluence correction of unity be applied in the transfer of dose to acrylic to the dose to water.

Because the pattern of dose buildup and $d_{\max}$ are affected by the spectrum of electrons incident upon the phantom, the scaling factors given in Sec. IV B, which are applicable to d_{50}, may not be applicable in the plateau region. The dose to water calculated from Eq. (19) is at $d_{\max}$ in water, but the exact depth of this $d_{\max}$ should be determined from depth-dose measurements made in water.

The SSD and collimator field size for electron dosimetry in a plastic phantom should be the same as for a water phantom.

VI. CALIBRATION OF ^{60}Co TELETHERAPY UNITS

A. In-air calibration

The absorbed dose at a point in a water phantom may be determined from the in-air exposure produced by a ^{60}Co teletherapy unit. Starting with an exposure-calibrated ionization chamber (Sec. II), this is essentially a three-step process:

(1) Measurement of the exposure at the SSD plus 0.5 cm, or at the isocenter of the ^{60}Co unit:

$$X = M N_X A_{\text{ion}} P_{\text{ion}}, \tag{20}$$

where M is the electrometer reading for the calibration field size (C or scale divisions) normalized to 22 °C and a pressure of one standard atmosphere, and N_X is the ^{60}Co exposure calibration factor (R/C or R/scale division).

(2) Calculation of the dose to a small mass of water of 0.5 cm radius at the reference distance:

$$D'_{\text{water}} = X f A_{\text{eq}}, \tag{21}$$

where f is the dose to water per roentgen of exposure, 0.967 cGy/R,[15] and A_{eq} is a factor that accounts for attenuation and scattering in the small mass of water, 0.989.[39]

TABLE XVI. Ratios of electron fluences at $d_{\max}$, water/polystyrene.

$\bar{E}_0$ (MeV)	$\phi^{\text{water}}_{\text{med}}$
5	1.039
7	1.033
10	1.025
13	1.017
16	1.009

(3) Application of the field-size-dependent backscatter factor (BSF), or 0.5-cm-depth tissue–air ratio ($\text{TAR}_{0.5}$) to obtain the dose to water at $d_{\max}$ in a full phantom:

$$D_{\text{water}} = D'_{\text{water}} (\text{BSF or } \text{TAR}_{0.5}). \tag{22}$$

These steps are combined in the following equation:

$$D_{\text{water}} = M N_X f A_{\text{eq}} (\text{BSF or } \text{TAR}_{0.5}). \tag{23}^{\ddagger}$$

B. Water-phantom calibration using N_D

The dose at a point in a water phantom may be measured with an ionization chamber having an absorbed-dose calibration factor for ^{60}Co gamma rays (Sec. II F). In this case, the chamber with appropriate waterproofing (which is not required for the NBS absorbed-dose calibration) is located at a depth of 5.0 cm in a water phantom. The center of the chamber should be at the treatment SSD plus 5.0 cm, or at the isocenter. The dose to water at $d_{\max}$ with the chamber removed is given by

$$D_{\text{water}} = \frac{M N_D}{P/100} \quad \text{or} \quad M N_D \left(\frac{\text{TAR}_{0.5}}{\text{TAR}_{5.0}}\right), \tag{24}^{\ddagger}$$

where N_D is the absorbed-dose calibration factor at a depth of 5 cm for ^{60}Co gamma rays incident upon water (cGy/C or cGy/scale division); P is the percent depth dose at 5-cm depth for the SSD and field size employed; $\text{TAR}_{0.5}$ is the tissue–air ratio at 0.5-cm depth and the field size employed; $\text{TAR}_{5.0}$ is the tissue–air ratio at 5.0-cm depth and the field size employed.

VII. GENERAL CONSIDERATIONS

A. Choice of ionization chamber

The uncertainty in the determination of absorbed dose to the dosimetry phantom is affected by the composition and geometry of the ionization chamber. The radiation field in the gas-filled cavity will be more like that in the phantom after the chamber is removed if the chamber is constructed from the same material as the phantom, or from a material whose radiation-absorption properties are very nearly the same. When the chamber composition is different from that of the phantom, e.g., an acrylic chamber in a water phantom, the wall thickness of the chamber should be as thin as possible, consistent with mechanical integrity. A buildup cap should not be used unless it is of the same composition as the phantom.

Most ionization chambers used in radiological physics have cylindrical or plane-parallel geometries. There are advantages and disadvantages of each type depending upon the application. Either type may be used for radiation dosimetry within the restrictions listed in Secs. II and V. Chambers of the plane-parallel design have replacement factors P_{repl} that are essentially unity, and the depth of measurement is well

‡ The product $A_{\text{ion}} P_{\text{ion}}$ is omitted from these expressions because the exposure rates [Eq. (23)] and dose rates [Eq. (24)] of cobalt teletherapy units are comparable to those produced by the calibration units, and $A_{\text{ion}} P_{\text{ion}}$ will be very close to unity.

defined at the inner surface of the proximal electrode. There are far fewer plane-parallel chambers in general use than cylindrical chambers, and their ^{60}Co exposure calibration, although achievable in principle, is not as yet a routine procedure at the calibration laboratories. Cylindrical chambers require gradient corrections on the order of 0.99 when used on the descending portion of photon-beam depth-dose curves, and electron fluence corrections on the order of 0.98 when used at d_{max} for electron beams. These corrections notwithstanding, cylindrical chambers are widely used, have a long history of reproducible exposure calibrations, and have been instrumental in establishing the traceability of clinical dosimetry to a national standard.

B. N_{gas} for plane-parallel chambers

It is recognized that cylindrical ionization chambers are widely used, and that the procedures for their in-air exposure calibration are firmly established. The same cannot yet be said for chambers of the plane-parallel design. Plane-parallel chambers that do not have NBS or ADCL calibrations may be used to verify the calibration of the lower range of electron energies from an accelerator when the higher energies can be calibrated with a cylindrical chamber whose P_{repl} is no smaller than 0.99. N_{gas} for a plane-parallel chamber may be determined as follows.

Using the highest electron-beam energy available and the cylindrical chamber for which N_{gas} is known, determine the response per monitor unit at d_{max}. Next, place the plane-parallel chamber into the same dosimetry phantom taking care to position the inner surface of its proximal electrode at the depth of the central axis of the cylindrical chamber, and determine its response per monitor unit. The cavity-gas calibration factor for the plane-parallel chamber is given by

$$(N_{gas})^{p\text{-}p} = \frac{(M N_{gas} P_{ion} P_{repl})^{cylin}}{(M P_{ion})^{p\text{-}p}}, \quad (25)$$

where the terms in the numerator apply to the cylindrical chamber, and those in the denominator apply to the plane-parallel chamber.

C. Dose to tissues

Computerized tomography has revealed that there are subtle variations from patient to patient in density and atomic composition of supposedly similar tissues. As the means to take account of these variations and include them into the treatment-planning process are now at hand, there is scant justification for assuming that tumors and intervening tissues all have the composition and density of ICRU muscle.[34] For this reason, the Protocol recommends that the calibration of radiation-therapy machines be expressed in terms of absorbed dose to water, and that the doses to various tissues be determined as part of the treatment-planning process.

D. Alternate dosimetric methods

It is recommended that, whenever possible, the beam calibration obtained by the method of the calibrated cavity (this Protocol) be confirmed by alternate, independent methods. At the present time, alternate methods are limited to calorimetry, the Fricke ferrous-sulfate dosimeter, and ionization measurements made with a chamber having an accurately known collecting volume.

1. Calorimeters

Calorimeters, which are generally regarded as giving the most accurate results, are made of graphite,[40,41] have an intricate construction with vacuum insulation, must be temperature stabilized prior to use, and are not suitable for routine beam calibration. Water calorimeters[42,52] are considerably easier to construct and operate, and offer the possibility of becoming a general-purpose dosimeter; at the time of this writing, the accuracy has not been established to the extent that water calorimeters can be regarded as acceptable for clinical dosimetry.

2. The Fricke ferrous-sulfate dosimeter

The Fricke ferrous-sulfate dosimeter offers many advantages over ionization chambers for high-energy radiation dosimetry: its composition is very close to that of water so that the dose to the dosimeter solution may be taken to be the dose to water; if thin-walled, low-density irradiation vessels are used, replacement corrections are not required; the response of the Fricke dosimeter is dose-rate independent; it does not require calibration at a national or regional laboratory. Some of the disadvantages of the Fricke dosimeter are an ultraviolet spectrophotometer is required for readout; exceptional care and cleanliness are required for consistent, accurate results; there are uncertainties in the ferric-ion yields (G values) on the order of $\pm$ 3%; more time is required for a dose determination; it cannot be regarded as a field instrument; doses of about 1000 cGy are required for accurate results even when 5-cm cuvettes are used for readout. The theory and application of chemical dosimeters has been described by Fricke and Hart.[43]

3. Independent ionization chambers

An uncalibrated ionization chamber may be used to confirm absorbed dose if its collecting volume is known with an uncertainty comparable to that of N_{gas} for the same chamber. Collecting volumes for cylindrical chambers are difficult to determine because of the complex shape of the electric field where the central electrode emerges from the insulator, and the difficulty of measuring internal dimensions. The collecting volumes of guarded field, plane-parallel chambers can be accurately controlled during fabrication, and the plate spacing subsequently checked by capacitance measurements if the collecting-plate area is known. The design, construction, and testing of independent plane-parallel chambers has been described by Holt *et al.*[17]

The cavity-gas calibration factor N_{gas} (Gy/C) for an independent ionization chamber is given by

$$N_{gas} = \frac{W/e}{V \times \rho}, \quad (26)$$

where V is the collecting volume (m^3) and ρ is the density of the gas at 22 °C and 760 mmHg (kg/m^3).

Equation (9) is then used to determine the dose to the dosimetry phantom from high-energy x rays or electrons.

VIII. APPLICATION OF THE PROTOCOL

A. Summary

(a) This Protocol covers the calibration of the following radiation beams: cobalt-60 gamma rays, x rays with nominal accelerating potentials in the range of 2–50 MV, and electrons with mean incident energies in the range of 5–50 MeV.

(b) The primary dosimeter shall be an ionization chamber having a calibration factor for ^{60}Co gamma rays directly traceable to NBS. The recommended ionization chambers are of the (i) plane-parallel design with electrode spacing and collecting electrode diameter not to exceed 2 mm and 2.6 cm, respectively; (ii) cylindrical design with internal diameters less than 1 cm. Whenever possible, ionization chambers should be constructed of the same material as the phantom.

(c) The Protocol recommends that beam calibrations be expressed in terms of dose to water. Water, polystyrene, or acrylic phantoms may be used. When plastic phantoms are used, various scaling and dose-transfer factors must be employed to obtain the dose to water. The dimensions of the phantom should be such that a 5-cm margin is present with the largest field size. Also, at least 10 cm of material beyond the dosimeter is necessary to assure maximum scatter.

(d) The measurement depths for beam calibration shall be (i) depth of dose maximum or on the exponentially decreasing portion of the depth-dose curve for photons, and (ii) depth of dose maximum for electrons. The depth chosen for photons is dependent on the internal dimensions of the ionization chamber.

B. Application

The application of the Protocol for calibration of high-energy radiation beams is essentially a two-step process. First, the dose to gas (air) in the chamber is determined; this is the product of the cavity-gas calibration factor N_{gas} and the electrometer reading corrected for ion recombination. (N_{gas} may be calculated using the ^{60}Co calibration factor and other data given in Sec. III, or it may be provided by the calibration laboratory.) Second, the dose to water from photon or electron beams is calculated using the methods and data of Secs. IV and V.

1. Calculation of the cavity-gas calibration factor N_{gas}

The ^{60}Co exposure calibration factor and N_{gas} will normally be provided by the calibration laboratory. Occasions may arise when the user is required to calculate N_{gas}. Worksheet (1), which can aid the user in making these calculations, has entry spaces for each of the required physical parameters, and references to where these data can be found in the Protocol. In addition, there is an Example Worksheet (1) with sample data for the calculation of N_{gas} for a typical ionization chamber, and Table XVII lists physical parameters and the ratios of N_{gas}/N_X for a group of commonly employed chambers.

2. Calculation of dose to water from photon beams

Worksheet (2) is used for ^{60}Co and x-ray dosimetry, and a new sheet should be used each time a dose calibration is made. Fractional depth dose may be replaced by tissue-maximum ratio (TMR) in the calibration of machines used for isocentric treatments. An example is given of the application of Worksheet (2) to the calibration of an x-ray beam with a stated energy of 4 MeV.

3. Calculation of dose to water from electron beams

Worksheet (3) is used for electron-beam dosimetry, and a new sheet should be used each time a dose calibration is made. An example is given of the application of Worksheet (3) to the calibration of an electron beam with a stated energy of 13 MeV.

TABLE XVII. Calculated ratios of N_{gas}/N_X for commonly employed ionization chambers (N_X is the exposure calibration factor for ^{60}Co gamma rays).

Chamber	A_{wall}	α	$(\bar{L}/\rho)^{wall}_{air}$	$(\bar{\mu}_{en}/\rho)^{air}_{wall}$	$(\bar{L}/\rho)^{cap}_{air}$	$(\bar{\mu}_{en}/\rho)^{air}_{cap}$	N_{gas}/N_X(Gy/R)[a]
Capintec–Farmer 0.6 cm^3, graphite wall, acrylic cap	0.990	0.42	1.010	0.999	1.103	0.925	8.52×10^{-3}
Capintec 0.1 cm^3, graphite wall, acrylic cap	0.991	0.90	1.010	0.999	1.103	0.925	8.57×10^{-3}
PTW normal, acrylic	0.994	1	1.103	0.925			8.51×10^{-3}
PTW transit, acrylic	0.994	1	1.103	0.925			8.51×10^{-3}
PTW micro, acrylic	0.988	1	1.103	0.925			8.46×10^{-3}
Shonka 0.1 cm^3, acrylic	0.989	1	1.103	0.925			8.47×10^{-3}
Exradin T.E. (A-150)	0.983	1	1.145	0.906			8.28×10^{-3}
Exradin A.E. (C-552)	0.973	1	1.000	1.000			8.50×10^{-3}
Far West IC-18 (A-150)	0.989	1	1.145	0.906			8.33×10^{-3}
Capintec parallel plate, polystyrene	0.995	0			1.112	0.928	8.43×10^{-3}

[a] For these calculated values of N_{gas}/N_X the ionization collection efficiency A_{ion} was assumed to be 1.00, and the quotient of absorbed dose by the collision fraction of kerma was taken to be 1.005.

Worksheet (1) for calculating the cavity-gas calibration factor N_{gas}

Name: _____ Date: _____

The cavity gas calibration factor is obtained from Eq. (6):

$$N_{gas} = N_X \frac{k\,(W/e) A_{ion}\, A_{wall}\, \beta_{wall}}{\alpha(\bar{L}/\rho)^{wall}_{air}(\bar{\mu}_{en}/\rho)^{air}_{wall} + (1-\alpha)(\bar{L}/\rho)^{cap}_{air}(\bar{\mu}_{en}/\rho)^{air}_{cap}}.$$

When chamber wall and buildup cap are of the same material, $\alpha = 1.00$.
When chamber wall and buildup cap are of different materials, α is obtained from Fig. 1.

1. (a) Chamber model and serial number: _____
   (b) Cavity inside diameter: _____ mm
   (c) Wall material and thickness: _____ g/cm^2
   (d) Buildup cap material and total wall plus cap thickness: _____ g/cm^2
   (e) Polarizing potential: _____ V

2. (a) Calibration laboratory and date: _____
   (b) Cobalt-60 exposure calibration factor at 22 °C and 1 atmosphere:

$N_X =$ _____ R/C

or $N_X =$ _____ R/scale division

3. (a) Charge per unit mass of air per unit exposure: $k = 2.58 \times 10^{-4}$ C/kg R
   (b) Average energy per unit charge: $W/e = 33.7$ J/C
   (c) Absorbed dose/collision fraction of kerma: $\beta_{wall} = 1.005$

4. (a) Ion-collection efficiency (obtained from NBS or ADCL, Sec. III D): $A_{ion} =$ _____
   (b) Wall-correction factor (Tables II or III): $A_{wall} =$ _____
   (c) Fraction of ionization due to electrons from chamber wall (Fig. 1): $\alpha =$ _____
   (d) Stopping-power ratio, wall/air (Table I): $(\bar{L}/\rho)^{wall}_{air} =$ _____
   (e) Energy-absorption coefficient ratio, air/wall (Table I): $(\bar{\mu}_{en}/\rho)^{air}_{wall} =$ _____
   (f) Fraction of ionization due to electrons from buildup cap: $(1-\alpha) =$ _____
   (g) Stopping-power ratio, cap/air (Table I): $(\bar{L}/\rho)^{cap}_{air} =$ _____
   (h) Energy-absorption coefficient ratio, air/cap (Table I): $(\bar{\mu}_{en}/\rho)^{air}_{cap} =$ _____

5. Cavity-gas calibration factor at 22 °C and 1 atmosphere:

$N_{gas} =$ _____ Gy/C

or $N_{gas} =$ _____ Gy/scale division

Example Worksheet (1) for calculating the cavity-gas calibration factor N_{gas}

Name: *John Doe* Date: *10 January 1984*

The cavity gas calibration factor is obtained from Eq. (6):

$$N_{gas} = N_X \frac{k(W/e)A_{ion}\, A_{wall}\, \beta_{wall}}{\alpha(\bar{L}/\rho)^{wall}_{air}(\bar{\mu}_{en}/\rho)^{air}_{wall} + (1-\alpha)(\bar{L}/\rho)^{cap}_{air}(\bar{\mu}_{en}/\rho)^{air}_{cap}}.$$

When chamber wall and buildup cap are of the same material, $\alpha = 1.00$.
When chamber wall and buildup cap are of different materials, α is obtained from Fig. 1.

1. (a) Chamber model and serial number: *PTW Normal, SN 123*
   (b) Cavity inside diameter: *5.0* mm
   (c) Wall material and thickness: *Acrylic, 0.42* g/cm^2
   (d) Buildup cap material and total wall plus cap thickness: *none* g/cm^2
   (e) Polarizing potential: *±350* V

2. (a) Calibration laboratory and date: *NBS 7 April 1982*
   (b) Cobalt-60 exposure calibration factor at 22 °C and 1 atmosphere:
   $N_X =$ *6.30×10^9* R/C
   or $N_X =$ _____ R/scale division

3. (a) Charge per unit mass of air per unit exposure: $k = 2.58\times10^{-4}$ C/kg R
   (b) Average energy per unit charge: $W/e = 33.7$ J/C
   (c) Absorbed dose/collision fraction of kerma: $\beta_{wall} = 1.005$

4. (a) Ion-collection efficiency (obtained from NBS or ADCL, Sec. III D): $A_{ion} =$ *0.993*
   (b) Wall-correction factor (Tables II or III): $A_{wall} =$ *0.994*
   (c) Fraction of ionization due to electrons from chamber wall (Fig. 1): $\alpha =$ *1.00*
   (d) Stopping-power ratio, wall/air (Table I): $(\bar{L}/\rho)^{wall}_{air} =$ *1.103*
   (e) Energy-absorption coefficient ratio, air/wall (Table I): $(\bar{\mu}_{en}/\rho)^{air}_{wall} =$ *0.925*
   (f) Fraction of ionization due to electrons from buildup cap: $(1-\alpha) =$ *0*
   (g) Stopping-power ratio, cap/air (Table I): $(\bar{L}/\rho)^{cap}_{air} =$ ...
   (h) Energy-absorption coefficient ratio, air/cap (Table I): $(\bar{\mu}_{en}/\rho)^{air}_{cap} =$ ...

5. Cavity-gas calibration factor at 22 °C and 1 atmosphere:
   $N_{gas} =$ *5.33×10^7* Gy/C
   or $N_{gas} =$ _____ Gy/scale division

Worksheet (2) for calculating the dose to water at d_{max} from photon beams

Name: _____ Date: _____

1. Radiation source: _____; Stated energy: _____ MeV

   Ionization ratio: _____ (Sec. IV B) Nominal accelerating potential: _____ MV (Fig. 3)

2. Phantom material (med): _____ SSD: _____ cm

   Collimator field size: _____ cm^2; Depth of measurement: _____ cm

3.1. Dose to phantom material per monitor unit [Eq. (9)]:

$$D_{med}/U = (\overline{M/U})\, N_{gas} (\bar{L}/\rho)^{med}_{air} P_{wall} P_{ion} P_{repl},$$

where U refers to accelerator monitor units, or time for a ^{60}Co unit.

3.2. The chamber temperature $T =$ _____ °C and pressure $P =$ _____ mmHg at the time of measurement. The chamber signal M is normalized to 22 °C and 1 atmosphere using the factor:

$$\frac{T + 273\ °C}{295\ °C} \times \frac{760\ mmHg}{P} = \_\_\_\_\_$$

3.3. Mean chamber signal per monitor unit (at the higher collecting potential, and normalized to 22 °C and 760 mmHg)

$(\overline{M/U}) =$ _____ C/monitor unit

or $(\overline{M/U}) =$ _____ scale division/monitor unit

3.4. Cavity-gas calibration factor:

Chamber model: _____ Wall material: _____

Inner diameter: _____ mm Wall thickness: _____ g/cm^2

$N_{gas} =$ _____ Gy/C or Gy/scale division.

3.5. Stopping-power ratio (Fig. 2, Table IV): $(\bar{L}/\rho)^{med}_{air} =$ _____

3.6. Wall correction factor [Eq. (10)]:

$$P_{wall} = \frac{[\alpha(\bar{L}/\rho)^{wall}_{air}(\bar{\mu}_{en}/\rho)^{med}_{wall} + (1-\alpha)(\bar{L}/\rho)^{med}_{air}]}{(\bar{L}/\rho)^{med}_{air}} = \_\_\_\_\_$$

Fraction of ionization from chamber wall (Fig. 7): $\alpha =$ _____

If $\alpha \geqslant 0.25$, enter α and $(1-\alpha)$. $(1-\alpha) =$ _____

If $\alpha < 0.25$, enter $\alpha = 0$ and proceed to 4.

Stopping-power ratio (Fig. 2, Table IV): $(\bar{L}/\rho)^{wall}_{air} =$ _____

Energy-absorption coefficient ratio (Table IX):

$(\bar{\mu}_{en}/\rho)^{med}_{air}$ _____ $\div$ $(\bar{\mu}_{en}/\rho)^{wall}_{air}$ _____ $= (\bar{\mu}_{en}/\rho)^{med}_{wall}$ _____

4. Ionization recombination correction (Sec. IV C and Fig. 4): $P_{ion} =$ _____

5. Replacement (gradient) correction (Fig. 5): $P_{repl} =$ _____

6. Dose to phantom material per monitor unit or per unit time,‖ at point of measurement: $D_{med}/U =$ _____ Gy/monitor unit

7.1. Dose to water per monitor unit, at d_{max} [Eq. (17)]:

$$D_{water}(\text{at } d_{max})/U = \frac{(D_{med}/U) \times ESC \times (\bar{\mu}_{en}/\rho)^{water}_{med}}{P/100}$$

7.2. Correction for excess scatter from acrylic phantoms (Table XIV): ESC = _____

7.3. Energy-absorption coefficient ratio (Table XII): $(\bar{\mu}_{en}/\rho)^{water}_{med} =$ _____

7.4. Percent depth dose at depth of measurement: $P =$ _____ %

7.5. Dose to water per monitor unit, at d_{max}: $D_{water}(\text{at } d_{max})/U =$ _____ Gy/monitor unit

‖ Cobalt-60 units may have a nonlinear relationship between dose per unit time and time, especially for short exposure times. Corrections should be made using the method of Orton and Siebert (Ref. 58).

Example Worksheet (2) for calculating the dose to water at d_{max} from photon beams

Name: *John Doe* Date: *7 May 1984*

1. Radiation source: *Clinac 4*; Stated energy: *4* MeV
   Ionization ratio: *0.630* (Sec. IV B) Nominal accelerating potential: *3.6* MV (Fig. 3)
2. Phantom material (med): *Polystyrene* SSD: *80* cm
   Collimator field size: *10×10* cm²; Depth of measurement: *5.0* cm
3.1 Dose to phantom material per monitor unit [Eq. (9)]:

$$D_{med}/U = (\overline{M/U})\, N_{gas} (\bar{L}/\rho)^{med}_{air} P_{wall} P_{ion} P_{repl},$$

where U refers to accelerator monitor units, or time for a ^{60}Co unit.

3.2. The chamber temperature $T =$ *25.0* °C and pressure $P =$ *758* mmHg at the time of measurement. The chamber signal M is normalized to 22 °C and 1 atmosphere using the factor:

$$\frac{T + 273\,°C}{295\,°C} \times \frac{760\ mmHg}{P} = \textit{1.013}$$

3.3. Mean chamber signal per monitor unit (at the higher collecting potential, and normalized to 22 °C and 760 mmHg)

$(\overline{M/U}) =$ *1.38×10⁻¹⁰* C/monitor unit

or $(\overline{M/U}) =$ _____ scale division/monitor unit

3.4. Cavity-gas calibration factor:

Chamber model: *PTW Normal* Wall material: *Acrylic*
Inner diameter: *5.0* mm Wall thickness: *0.42* g/cm²

$N_{gas} =$ *5.33×10⁷* Gy/C or Gy/scale division.

3.5. Stopping-power ratio (Fig. 2, Table IV): $(\bar{L}/\rho)^{med}_{air} =$ *1.110*

3.6. Wall correction factor [Eq. (10)]:

$$P_{wall} = \frac{[\alpha(\bar{L}/\rho)^{wall}_{air}(\bar{\mu}_{en}/\rho)^{med}_{wall} + (1-\alpha)(\bar{L}/\rho)^{med}_{air}]}{(\bar{L}/\rho)^{med}_{air}} = \textit{0.990}$$

Fraction of ionization from chamber wall (Fig. 7): $\alpha =$ *0.93*
If $\alpha \geqslant 0.25$, enter α and $(1-\alpha)$. $(1-\alpha) =$ *0.07*
If $\alpha < 0.25$, enter $\alpha = 0$ and proceed to 4.

Stopping-power ratio (Fig. 2, Table IV): $(\bar{L}/\rho)^{wall}_{air} =$ *1.101*

Energy-absorption coefficient ratio (Table IX):

$(\bar{\mu}_{en}/\rho)^{med}_{air}$ *1.072* $\div (\bar{\mu}_{en}/\rho)^{wall}_{air}$ *1.077* $= (\bar{\mu}_{en}/\rho)^{med}_{wall}$ *0.997*

4. Ionization recombination correction (Sec. IV C and Fig. 4): $P_{ion} =$ *1.011*
5. Replacement (gradient) correction (Fig. 5): $P_{repl} =$ *0.994*
6. Dose to phantom material per monitor unit or per unit time,** at point of measurement: $D_{med}/U =$ *8.12×10⁻³* Gy/monitor unit

7.1. Dose to water per monitor unit, at d_{max} [Eq. (17)]:

$$D_{water}(\text{at } d_{max})/U = \frac{(D_{med}/U) \times ESC \times (\bar{\mu}_{en}/\rho)^{water}_{med}}{P/100}$$

7.2. Correction for excess scatter from acrylic phantoms (Table XIV): ESC = ...

7.3. Energy-absorption coefficient ratio (Table XII): $(\bar{\mu}_{en}/\rho)^{water}_{med} =$ *1.036*

7.4. Percent depth dose at depth of measurement: $P =$ *82.4* %

7.5. Dose to water per monitor unit, at d_{max}: $D_{water}(\text{at } d_{max})/U =$ *1.02×10⁻²* Gy/monitor unit

**Cobalt-60 units may have a nonlinear relationship between dose per unit time and time, especially for short exposure times. Corrections should be made using the method of Orton and Siebert (Ref. 58).

Worksheet (3) for calculating the dose to water at d_{max} from electron beams

Name: _____ Date: _____

1. Radiation source: _____; Stated energy: _____ MeV

   d_{50} _____ cm water (Sec. IV B) Mean incident energy ($\bar{E}_0$): _____ MeV (Sec. IV B)

2. Phantom material (med): _____ SSD: _____ cm

   Collimator field size: _____ cm^2 Depth of measurement: _____ cm Practical range R_p _____ cm

   Mean energy at measurement depth $\bar{E}_z$ (Table VIII): _____ MeV

3.1. Dose to phantom material per monitor unit [Eq. (9)]:

$$D_{med}/U = (\overline{M/U})N_{gas}(\bar{L}/\rho)^{med}_{air}P_{ion}\,P_{repl},$$

where U refers to accelerator monitor units.

3.2. The chamber temperature $T =$ _____ °C and pressure $P =$ _____ mmHg at the time of measurement. The chamber signal M is normalized to 22 °C and 1 atmosphere, using the factor

$$\frac{T + 273\,°C}{295\,°C} \times \frac{760\ mmHg}{P} = \_\_\_\_\_$$

3.3. Mean chamber signal per monitor unit (at the higher collecting potential, and normalized to 22 °C and 760 mmHg).

$(\overline{M/U}) =$ _____ C/monitor unit

or $(\overline{M/U}) =$ _____ scale division/monitor unit

3.4. Cavity-gas calibration factor:

Chamber model: _____ Inner diameter: _____ mm

$N_{gas} =$ _____ Gy/C or Gy/scale division

3.5. Stopping power ratio for $\bar{E}_0$ at depth (Tables V–VII): $(\bar{L}/\rho)^{med}_{air} =$ _____

4. Ionization recombination correction (Sec. IV C and Fig. 4): $P_{ion} =$ _____

5. Replacement (electron fluence) correction (Table VIII): $P_{repl} =$ _____

6. Dose to phantom material per monitor unit, at point of measurement: $D_{med}/U =$ _____ Gy/monitor unit

7.1. Dose to water per monitor unit, at d_{max} [Eq. (19)]:

$$D_{water}\ (\text{at}\ d_{max})/U = (D_{med}/U)(\bar{S}/\rho)^{water}_{med}\,\phi^{water}_{med}$$

7.2. Unrestricted stopping-power ratio (Table XV): $(\bar{S}/\rho)^{water}_{med}$ _____

7.3. Electron fluence correction (Table XVI): ϕ^{water}_{med} _____

7.4. Dose to water per monitor unit, at d_{max}: $D_{water}\ (\text{at}\ d_{max})/U =$ _____ Gy/monitor unit

Example Worksheet (3) for calculating the dose to water at d_{max} from electron beams

Name: *John Doe* Date: *6 June 1984*

1. Radiation source: *Sagittaire* ; Stated energy: *13* MeV
   d_{50} *5.25* cm water (Sec. IV B) Mean incident energy ($\bar{E}_0$): *12.2* MeV (Sec. IV B)
2. Phantom material (med): *Polystyrene* SSD: *105* cm
   Collimator field size: *10×10* cm^2 Depth of measurement: *2.75* cm Practical range R_p *6.12* cm
   Mean energy at measurement depth $\bar{E}_z$ (Table VIII): *6.72* MeV
3.1. Dose to phantom material per monitor unit [Eq. (9)]:

$$D_{med}/U = (\overline{M/U})N_{gas}(\bar{L}/\rho)^{med}_{air}P_{ion}\,P_{repl},$$

where U refers to accelerator monitor units.

3.2. The chamber temperature $T =$ *23.5* °C and pressure $P =$ *765* mmHg at the time of measurement. The chamber signal M is normalized to 22 °C and 1 atmosphere, using the factor

$$\frac{T + 273\,°C}{295\,°C} \times \frac{760\ mmHg}{P} = \textit{1.00}$$

3.3. Mean chamber signal per monitor unit (at the higher collecting potential, and normalized to 22 °C and 760 mmHg).

$(\overline{M/U}) =$ *1.16×10⁻¹⁰* C/monitor unit

or $(\overline{M/U}) =$ _____ scale division/monitor unit

3.4. Cavity-gas calibration factor:

Chamber model: *Farmer Graphite* Inner diameter: *6.0* mm

$N_{gas} =$ *5.42×10⁷* Gy/C or Gy/scale division

3.5. Stopping power ratio for $\bar{E}_0$ at depth (Tables V–VII): $(\bar{L}/\rho)^{med}_{air} =$ *1.003*

4. Ionization recombination correction (Sec. IV C and Fig. 4): $P_{ion} =$ *1.020*

5. Replacement (electron fluence) correction (Table VIII): $P_{repl} =$ *0.971*

6. Dose to phantom material per monitor unit, at point of measurement: $D_{med}/U =$ *6.25×10⁻³* Gy/monitor unit

7.1. Dose to water per monitor unit, at d_{max} [Eq. (19)].

$$D_{water}\ (\text{at } d_{max})/U = (D_{med}/U)(\bar{S}/\rho)^{water}_{med}\,\phi^{water}_{med}$$

7.2. Unrestricted stopping-power ratio (Table XV): $(\bar{S}/\rho)^{water}_{med}$ *1.030*

7.3. Electron fluence correction (Table XVI): ϕ^{water}_{med} *1.020*

7.4. Dose to water per monitor unit, at d_{max}: $D_{water}\ (\text{at } d_{max})/U =$ *6.56×10⁻³* Gy/monitor unit

ACKNOWLEDGMENTS

The authors of this Protocol appreciate fully that the steps they have taken to advance the practice of radiation dosimetry rest upon decades of theoretical and experimental research by physicists the world over, and upon the various handbooks, codes of practice, and protocols written by comparable professional groups. Specific mention is due to Martin Berger of NBS who supplied the Task Group with up-to-date stopping-power data, and to Robert Loevinger whose Formalism for Calculation of Absorbed Dose to a Medium from Photon and Electron Beams provides the theoretical basis for the procedures of this Protocol. The Task Group is also indebted to Joseph Blinick, James Deye, Edward Epp, Douglas Jones, and James Purdy for their midcourse corrections of the Protocol, and to members of the Radiation Therapy Committee, the Radiological Physics Center, and the Centers of Radiological Physics for their reviews and comments of the final draft. The Task Group was encouraged to complete its task by Robert Morton of BDRH, and meetings, and technical and administrative support were financed by a BRH contract (FDA #223-80-6008). Travel funds that made it possible for the Task Group to meet during its early years were provided by the Radiological Physics Center from NCI Grant No. CA-10953. Last, but not least, we are gratefully indebted to Ann Marie DePetto for her endless patience, critical eye, and superb typing in the preparation of the manuscript.

[1]G. H. Fletcher, *Textbook of Radiotherapy*, 3rd ed. (Lea and Febiger, Philadelphia, 1981).
[2]ICRU Report No. 14, "Radiation Dosimetry: X-Rays and Gamma Rays with Maximum Photon Energies Between 0.6 and 50 MeV" (ICRU, Washington, D.C., 1969).
[3]A. E. Nahum and J. R. Greening, Phys. Med. Biol. **23**, 894 (1978).
[4]A. E. Nahum and J. R. Greening, Phys. Med. Biol. **21**, 862 (1976).
[5]G. Kutcher, K. Strubler, and N. Suntharalingam, Med. Phys. **4**, 414 (1977).
[6]P. R. Almond and H. Svensson, Acta Radiol. Ther. Phys. Biol. **16**, 177 (1977).
[7]Hospital Physicist's Association, Phys. Med. Biol. **14**, 1 (1969).
[8]ICRU Report No. 21, "Radiation Dosimetry: Electrons with Initial Energies Between 1 and 50 MeV" (ICRU, Washington, D.C., 1972).
[9]Nordic Association of Clinical Physics, Acta Radiol. Ther. Phys. Biol. (1971).
[10]Subcommittee on Radiation Dosimetry, AAPM, Phys. Med. Biol. **16**, 379 (1971).
[11]J. S. Pruitt, S. R. Domen, and R. Loevinger, J. Res. Natl. Bur. Stand. **86**, 495 (1981).
[12]T. E. Burlin, *Radiation Dosimetry* (Academic, New York, 1968), Vol. 1, p. 331.
[13]ICRU Report No. 31, "Average Energy Required to Produce an Ion Pair" (ICRU, Washington, D.C., 1979).
[14]T. P. Loftus and J. T. Weaver, J. Res. Natl. Bur. Stand. **78A**, 465 (1974).
[15]H. E. Johns and J. R. Cunningham, *The Physics of Radiology*, 4th ed. (Thomas, Springfield, Ill., 1983).
[16]W. H. Henry, Phys. Med. Biol. **24**, 37 (1979).
[17]J. G. Holt, A. Buffa, D. J. Perry, I-C. Ma, and J. C. MacDonald, Int. J. Radiat. Oncol. Biol. Phys. **5**, 2031 (1979).
[18]R. Nath and R. J. Schulz, Med. Phys. **8**, 85 (1981).
[19]R. Loevinger, Med. Phys. **8**, 1 (1981).
[20]G. Lempert, R. Nath, and R. J. Schulz, Med. Phys. **10**, 1 (1983).
[21]K. Johansson, L. Mattsson, L. Lindborg, and H. Svensson, IAEA-SM-222/35, Vienna, Austria, 1977.
[22]Nordic Association of Clinical Physics, Acta Radiol. Oncol. Radiat. Phys. Biol. **19**, 55 (1980).
[23]M. Berger (personal communication). Data available upon request from Dr. Berger, Radiation Physics Division, Center for Radiation Research, National Bureau of Standards, Washington, D.C. 20234.
[24]J. W. Boag, *Radiation Dosimetry* (Academic, New York, 1966), Vol. 2, p. 1.
[25]J. R. Cunningham and R. J. Schulz, Med. Phys. (submitted).
[26]J. R. Cunningham and M. R. Sontag, Med. Phys. **7**, 672 (1980).
[27]J. Dutreix and A. Dutreix, Biophysik **3**, 249 (1966).
[28]G. Hettinger, C. Petterson, and H. Svensson, Acta Radiol. **6**, 61 (1967).
[29]H. Weatherburn and B. Stedeford, Br. J. Radiol. **50**, 921 (1977).
[30]H. E. Johns and J. R. Cunningham, *The Physics of Radiology*, 3rd ed. (Thomas, Springfield, Ill., 1969).
[31]D. Harder, Biophysik **5**, 157 (1968).
[32]H. Svensson and A. Brahme, Acta Radiol. Oncol. **18**, 326 (1979).
[33]R. J. Schulz and R. Nath, Med. Phys. **6**, 153 (1979).
[34]ICRU Report No. 10b, "Physical Aspects of Irradiation," NBS Handbook No. 85 (ICRU, Washington, D.C., 1964).
[35]P. R. Almond, Med. Phys. **8**, 901 (1981).
[36]M. J. Berger and S. M. Seltzer, "Stopping Powers and Ranges of Electrons and Positrons," NBS IR 82-2550, U.S. Dept. of Commerce (1982).
[37]J. W. Boag, Phys. Med. Biol. **27**, 201 (1982); J. W. Boag and J. Currant, Br. J. Radiol. **53**, 471 (1980).
[38]J. H. Hubbell, Radiat. Res. **70**, 58 (1977).
[39]J. E. Bond, R. Nath, and R. J. Schulz, Med. Phys. **5**, 422 (1978).
[40]S. R. Domen and P. J. Lamperti, J. Res. Natl. Bur. Stand. **78A**, 595 (1974).
[41]J. S. Laughlin and S. Genna, *Radiation Dosimetry* (Academic, New York, 1966), Vol. 2, p. 389.
[42]S. R. Domen, Med. Phys. **7**, 157 (1980).
[43]H. Fricke and E. J. Hart, *Radiation Dosimetry* (Academic, New York, 1966), Vol. 2, p. 167.
[44]R. Loevinger, C. J. Karzmark, and M. Weissbluth, Radiology **77**, 906 (1961).
[45]M. J. Berger and S. M. Seltzer, Natl. Bur. Stand. (U.S.) Internal Report 82-2451, 1982.
[46]H. Casson, Med. Phys. **5**, 321 (1978) (abstract); (personal communication).
[47]L. O. Mattsson, K. A. Johansson, and H. Svensson, Acta Radiol. Oncol. **21** (1982).
[48]K. R. Hogstrom and P. R. Almond, abstract presented at the annual meeting of the AAPM, New Orleans; Med. Phys. **9**, 607 (1982).
[49]L. W. Berkley and W. F. Hanson, abstract presented at the annual meeting of the AAPM, New Orleans; Med. Phys. **9**, 607 (1982).
[50]J. S. Pruitt and R. Loevinger, Med. Phys. **9**, 176 (1982).
[51]NCRP Report No. 69, "Dosimetry of X-Ray and Gamma-Ray Beams for Radiation Therapy in the Energy Range 10 keV to 50 MeV" (NCRP, Washington, D.C., 1981).
[52]S. R. Domen, J. Res. Natl. Bur. Stand. **87**, 211 (1982).
[53]J. E. O'Connor, Phys. Med. Biol. **1**, 352 (1957).
[54]Subcommittee on Radiation Dosimetry, AAPM, Phys. Med. Biol. **11**, 505 (1966).
[55]K. R. Kase, G. J. Adler, and B. E. Bjärngard, Med. Phys. **9**, 13 (1982).
[56]S. C. Klevenhagen, G. D. Lambert, and A. Arbabi, Phys. Med. Biol. **27**, 363 (1982).
[57]Nordic Association of Clinical Physics, Acta Radiol. Oncol. Suppl. **20** (1981).
[58]C. R. Orton and J. Siebert, Phys. Med. Biol. **16**, 379 (1971).